



**HAL**  
open science

## Essential role of the plant DNA polymerase theta for the repair of replication-associated DNA damage under standard and abiotic stress conditions

Maherun Nisa, Clara Bergis, Jose-Antonio Pedroza-Garcia, Jeannine Drouin-Wahbi, Christelle Mazubert, Catherine Bergounioux, Moussa Benhamed, Cécile Raynaud

### ► To cite this version:

Maherun Nisa, Clara Bergis, Jose-Antonio Pedroza-Garcia, Jeannine Drouin-Wahbi, Christelle Mazubert, et al.. Essential role of the plant DNA polymerase theta for the repair of replication-associated DNA damage under standard and abiotic stress conditions. *The Plant Journal*, 2021, pp.1-40. 10.1111/tpj.15295 . hal-03240087

**HAL Id: hal-03240087**

**<https://hal.science/hal-03240087>**

Submitted on 27 May 2021

**HAL** is a multi-disciplinary open access archive for the deposit and dissemination of scientific research documents, whether they are published or not. The documents may come from teaching and research institutions in France or abroad, or from public or private research centers.

L'archive ouverte pluridisciplinaire **HAL**, est destinée au dépôt et à la diffusion de documents scientifiques de niveau recherche, publiés ou non, émanant des établissements d'enseignement et de recherche français ou étrangers, des laboratoires publics ou privés.



Distributed under a Creative Commons Attribution 4.0 International License

1 **Essential role of the plant DNA polymerase theta for the repair of replication-**  
2 **associated DNA damage under standard and abiotic stress conditions**

3 **Maherun Nisa<sup>1,2</sup>, Clara Bergis<sup>1,2</sup>, Jose-Antonio Pedroza-Garcia<sup>1,2</sup>, Jeannine Drouin-Wahbi<sup>1,2</sup>,**  
4 **Christelle Mazubert<sup>1,2</sup>, Catherine Bergounioux<sup>1,2</sup>, Moussa Benhamed<sup>1,2</sup> and Cécile Raynaud<sup>1,2</sup>**

5 **1 Université Paris-Saclay, CNRS, INRAE, Univ Evry, Institute of Plant Sciences Paris-Saclay**  
6 **(IPS2), 91405, Orsay, France.**

7 **2 Université de Paris, CNRS, INRAE, Institute of Plant Sciences Paris Saclay (IPS2) 91405 Orsay**

8 **Running head:** Role of DNA Pol  $\theta$  in the repair of replication associated DNA damage

9 **ABSTRACT**

10 Safeguard of genome integrity is a key process in all living organisms. Due to their sessile lifestyle,  
11 plants are particularly exposed to all kinds of stress conditions that could induce DNA damage.  
12 However, very few genes involved in the maintenance of genome integrity are indispensable to  
13 plants' viability. One remarkable exception is the *POLQ* gene that encodes DNA polymerase theta  
14 (Pol  $\theta$ ), a non-replicative polymerase involved in Trans-Lesion Synthesis (TLS) during DNA  
15 replication and Double-Strand Breaks (DSB) repair. The *Arabidopsis* *tebichi* (*teb*) mutants,  
16 deficient for Pol  $\theta$ , have been reported to display severe developmental defects, leading to the  
17 conclusion that Pol  $\theta$  is required for normal plant development. However, this essential role of Pol  
18  $\theta$  in plants is challenged by contradictory reports regarding the phenotypic defects of *teb* mutants,  
19 and the recent finding that rice null mutants develop normally. Here we show that the phenotype  
20 of *teb* mutants is highly variable. Taking advantage of hypomorphic mutants for the replicative  
21 DNA polymerase  $\epsilon$ , that display constitutive replicative stress, we show that Pol  $\theta$  allows  
22 maintenance of meristem activity when DNA replication is partially compromised. Furthermore,  
23 we found that the phenotype of Pol  $\theta$  mutants can be aggravated by modifying their growth  
24 conditions, suggesting that environmental conditions impact the basal level of replicative stress,  
25 and providing evidence for a link between plants' response to adverse conditions, and mechanisms  
26 involved in the maintenance of genome integrity.

27 **Key words:** Genome stability, DNA replication, Pol  $\theta$ , abiotic stress, plants

28 **Significance statement:** Pol  $\theta$  is one of the few proteins involved in DNA repair that appears to  
29 be essential for plant development, but there are contradictory reports concerning the phenotype  
30 of Pol  $\theta$ -deficient mutants. Here we show that Pol  $\theta$  plays a key role in the repair of replication-  
31 associated DNA breaks, and that its requirement for plant development depends on growth  
32 conditions, providing evidence for a link between abiotic stress responses and the DNA Damage  
33 Response.

34

## 35 INTRODUCTION

36 Organism's survival depends on the faithful transmission of genetic information. Due to their  
37 sessile lifestyle, plants cannot escape stress conditions with the potential to compromise their  
38 genome integrity. Indeed, because sunlight is the energy source of plants, they are constantly  
39 exposed to UV-radiations, that can cause DNA damage such as pyrimidine dimers. In addition,  
40 cellular metabolic activities such as photosynthesis lead to the production of Reactive Oxygen  
41 Species (Noctor and Foyer, 2016), that can induce DNA lesions, and whose production can be  
42 exacerbated by various biotic and abiotic stress conditions. In plants like in all eukaryotes, DNA  
43 lesions are recognized and trigger a signaling cascade called the DNA damage response (DDR)  
44 that leads to the activation of cell cycle checkpoints in proliferating cells, and specific DNA repair  
45 mechanisms (Ciccia and Elledge, 2010; Yoshiyama *et al.*, 2013; Hu *et al.*, 2016; Nisa *et al.*, 2019).  
46 Outcomes of DDR activation may be different depending on the severity of DNA damage and on  
47 the efficiency of the repair process: successful repair allows cell survival and resumption of the  
48 cell cycle, but if the damage is too severe, it may induce permanent cell proliferation arrest through  
49 endoreduplication (Adachi *et al.*, 2011) or even cell death (Fulcher and Sablowski, 2009). The  
50 cellular response also depends on the cell type, meristematic cells being more sensitive to DNA  
51 damage and more prone to undergo cell death than differentiated cells (Fulcher and Sablowski,  
52 2009).

53 Because maintenance of genome integrity relies on its faithful duplication in proliferating cells,  
54 and its efficient repair in all cell types, DNA polymerases (Pol) play a pivotal role in this process  
55 (Burgers, 1998). In eukaryotes, DNA polymerases are distributed between replicative and non-  
56 replicative polymerases (Burgers, 1998), and classified into 4 families (A, B, X and Y), based on  
57 the primary structure of their catalytic subunit (Makarova and Koonin, 2013). The three replicative  
58 polymerases (DNA Pol  $\alpha$ ,  $\delta$  and  $\epsilon$ ) belong to the B-family (Jain *et al.*, 2018) whereas non-  
59 replicative polymerases can be found in all families, and are involved in different DNA repair  
60 pathways. One distinctive feature of replicative polymerases is their tight catalytic sites that  
61 confers them a very low error rate (Kunkel, 2004). Consequently, their progression during DNA  
62 replication can be blocked by lesions that are too large to be accommodated in their catalytic site,  
63 such as bulky adducts or pyrimidine dimers. When replisome progression is prevented by a DNA  
64 lesion on the template strand, non-replicative polymerases that have a looser active site can



65 substitute for canonical replicative ones to perform Trans-Lesion Synthesis (TLS), a process by  
66 which they allow the replisome to progress beyond the DNA lesions (Kunkel, 2004; Yang and  
67 Gao, 2018). TLS polymerases are thought to associate into a huge complex with stalled replication  
68 forks, allowing the choice of the most appropriate one to bypass the lesion, depending on its nature  
69 (Powers and Washington, 2018). The high diversity of TLS polymerases likely stems from the fact  
70 that they have different so-called cognate lesions, opposite to which they are able to perform error-  
71 free DNA synthesis: each TLS polymerase can thus be recruited for efficient error-free bypass of  
72 specific lesions (Powers and Washington, 2018). Plant genomes encompass at least 9 non-  
73 replicative polymerases, 6 of which have been functionally characterized, and involved in TLS  
74 and/or DNA repair: Pol  $\zeta$ ,  $\eta$ ,  $\kappa$ ,  $\theta$ , and  $\lambda$  and Reversionless1 (Rev1) (reviewed in (Pedroza-Garcia  
75 *et al.*, 2019; Sakamoto, 2019)). Deficiency in non-replicative polymerases usually does not affect  
76 overall development, but rather results in hypersensitivity to various DNA-damaging agents  
77 (Pedroza-Garcia *et al.*, 2019). One intriguing exception is Pol  $\theta$  (encoded by the *POLQ* gene) also  
78 called TEBICHI in *Arabidopsis thaliana*: *teb* null mutants show severe developmental defects  
79 (Inagaki *et al.*, 2006; Inagaki *et al.*, 2009), suggesting that the cellular function of Pol  $\theta$  is essential  
80 for proper development.

81 The knowledge about the molecular function of Pol  $\theta$  in plants is scarce in comparison to other  
82 eukaryotes. In Human cells, Pol  $\theta$  can perform error-prone TLS through UV-lesions. Its deficiency  
83 results in a dramatic increase of tumorigenesis upon UV exposure, indicating that this error-prone  
84 TLS is crucial to avoid collapse of stalled forks (Yoon *et al.*, 2019). Another key function of Pol  
85  $\theta$  is DSB repair through ALternative Non-Homologous End Joining (Alt-NHEJ), also called  
86 Micro-homology Mediated End Joining (MMEJ) (Beagan and McVey, 2016). Alt-NHEJ is an  
87 error-prone pathway for DSB repair in which resection of DNA ends on each side of the break  
88 exposes micro-homology of only a few base pairs, that can allow annealing of single stranded  
89 DNA (ssDNA) and subsequent end-joining (Chiruvella *et al.*, 2013). Recently, Mateos-Gomez and  
90 colleagues demonstrated that through its helicase domain, Pol  $\theta$  facilitates the displacement of  
91 RPA that normally protects resected ends and promotes homologous recombination (HR), thereby  
92 favoring Alt-NHEJ over HR (Mateos-Gomez *et al.*, 2017).

93 This dual role of Pol  $\theta$  in DSB repair is likely a key factor of the cellular response to replicative  
94 (or replication) stress. Replicative stress is a complex phenomenon that arises when fork

95 progression is stopped or slowed-down. If the obstacle cannot be bypassed (for example through  
96 TLS), fork stalling triggers the accumulation of single stranded DNA coated by the replication  
97 protein RPA, leading to the activation of the ATR (ATM and Rad3-related) kinase and subsequent  
98 DDR signaling (reviewed in (Zeman and Cimprich, 2014)). Pol  $\theta$  is thus assumed both to prevent  
99 replicative stress by avoiding fork stalling at DNA lesions, and to contribute to DNA repair when  
100 replicative stress results in fork collapse and subsequent DSB formation. Indeed, in Human cells,  
101 *POLQ* deficiency confers hypersensitivity to ATR inhibitors, providing evidence for the role of  
102 Pol  $\theta$  for the repair of DNA replication-induced DNA damage (Wang *et al.*, 2019), and a synthetic  
103 lethal genetic screen revealed that various components of the DDR are indispensable to cell  
104 survival in the absence of Pol  $\theta$ . The common feature of all mutations identified in the screen was  
105 that they caused accumulation of endogenous DNA damage, indicating that the most prominent  
106 role of Pol  $\theta$  is the repair of replication-associated DSB, regardless of the initial cause of DNA  
107 damage (Feng *et al.*, 2019). There is thus accumulating evidence that Pol  $\theta$  is key for repairing  
108 DSBs associated with fork collapse due to replication stress, via Alt-NHEJ (Wang *et al.*, 2019;  
109 Kelso *et al.*, 2019). Analysis of plant Pol  $\theta$  mutants suggests that this dual role is conserved in  
110 plants. The *teb* mutants show constitutive activation of the DNA Damage Response (DDR),  
111 consistent with role of Pol  $\theta$  in the maintenance of genome integrity (Inagaki *et al.*, 2006). They  
112 are more sensitive to UV, and to the DNA alkylating agent methylmethane sulfonate (MMS)  
113 (Inagaki *et al.*, 2006), consistent with a TLS function. Furthermore, Pol  $\theta$ -dependent Alt-NHEJ  
114 was identified as the pathway for T-DNA integration after transformation by agrobacterium (van  
115 Kregten *et al.*, 2016), although this finding has lately been questioned by the observation that T-  
116 DNA integration remains possible, albeit with a reduced efficiency, in Pol  $\theta$  null mutants  
117 (Nishizawa-Yokoi *et al.*, 2020).

118 Two important questions still hold regarding the function of plant Pol  $\theta$ . First, it is not clear whether  
119 the TLS or DSB repair function, or both can account for the fact that this protein is required for  
120 normal plant development, as most plant mutants deficient for TLS or DNA repair develop  
121 normally in the absence of genotoxic stress. Second, there are conflicting reports regarding the  
122 developmental defects caused by Pol  $\theta$  deficiency, and it thus remains unclear to what extent it is  
123 indeed required for normal development. As mentioned above, several *teb* alleles (*teb1*, *teb2* and  
124 *teb5*) have been described in Arabidopsis and were all reported to display the same phenotypic

125 alterations including reduced growth, deformed leaves and disorganized root meristems (Inagaki  
126 *et al.*, 2006; Inagaki *et al.*, 2009). However, in *Physcomitrella patens*, *polq* mutants were deficient  
127 for DSB repair, but did not show any developmental defects (Mara *et al.*, 2019), and authors  
128 questioned the requirement of Pol  $\theta$  for normal development in Arabidopsis, as other groups did  
129 not seem to observe severe developmental defects (van Kregten *et al.*, 2016). More recently, *polq*  
130 mutants were generated in rice, and reported to develop normally under standard growth  
131 conditions, although regeneration from calli was severely impaired (Nishizawa-Yokoi *et al.*,  
132 2020).

133 To tackle these questions, we carefully re-examined the phenotype of *teb* mutants, finding that it  
134 is highly variable. Furthermore, to try and determine the origin of developmental defects caused  
135 by Pol  $\theta$  deficiency, we took advantage of the *pol2a-4* mutant that is partially deficient in the  
136 replicative polymerase Pol  $\epsilon$  and shows constitutive replicative stress (Pedroza-Garcia *et al.*,  
137 2017). Our results indicate that one key cellular function of Pol  $\theta$  is to avoid DNA damage  
138 accumulation during DNA replication, and that developmental defects observed in *teb* mutants are  
139 likely consequences of replicative stress. Finally, we show that the phenotype of *teb* mutants can  
140 be aggravated by exposure to abiotic stresses, suggesting that environmental conditions impact the  
141 basal level of replicative stress, and providing evidence for a link between plant tolerance to stress,  
142 and mechanisms involved in the maintenance of genome integrity.

## 143 **RESULTS**

144 Previous work reported the phenotype of *teb* mutants, with stunted growth and deformed leaves  
145 (Inagaki *et al.*, 2006). Five alleles of the mutant were initially described, three of which: *teb1*, *teb2*  
146 and *teb5* gave rise to the same phenotype and appeared to be full loss of function mutants (Inagaki  
147 *et al.*, 2006) (Figure 1A). However, rice mutants did not show developmental defects (Nishizawa-  
148 Yokoi *et al.*, 2020), and other groups reported much milder phenotypical defects for *teb2* and *teb5*  
149 mutants (van Kregten *et al.*, 2016). To clarify this, we carefully re-examined the phenotype of  
150 these mutants. In our growth conditions, most of the *teb2* and *teb5* mutants appeared  
151 indistinguishable from the wild-type after 1 month of growth (Figure 1B). We classified *teb*  
152 mutants' phenotypes in two categories: wild type like (WTL) plants appeared identical to the wild-  
153 type (Col-0) and plants with severe (S) developmental defects showed the previously described

154 *tebichi* phenotype (Figure 1B). We first checked that both WTL and S plants were homozygous  
155 for the *teb* mutation, using primers flanking the T-DNA insertions in *teb2* and *teb5* mutants (Figure  
156 1A, C). We also checked by qPCR that both *teb* alleles we used did not allow the expression of  
157 the full length *POLQ* mRNA. To this end we used three primer pairs: one (#1) at the 5' end of the  
158 *TEB* gene, upstream both insertions, one flanking the T-DNA insertion site of the *teb5* mutant (#2),  
159 and one (#3) in the 3' moiety of the gene (Figure 1A). The first primer pair allowed detection of  
160 wild-type levels of mRNA in both mutants, indicating that the 5' extremity of the gene is normally  
161 expressed (Figure 1D). However, the *teb2* mutant accumulated no detectable transcripts produced  
162 downstream of the insertion. Expression of the 3' moiety of the gene was drastically reduced in  
163 *teb5* and no mRNA spanning the insertion site could be detected (Figure 1D). Thus, neither *teb2*  
164 nor *teb5* accumulate full length *TEB* mRNA, and are likely knock-out mutants, consistent with  
165 previous reports (Inagaki *et al.*, 2006). We next quantified the distribution of *teb* mutants between  
166 the two phenotypic categories. In our growth conditions ~ 85-90% of *teb* mutants were in the WTL  
167 category and only 10% to 15% in the S category corresponding to the previously described  
168 phenotype (Figure 1E).

169 Since *teb* mutants were shown to display a constitutive upregulation of DNA damage responsive  
170 genes (Inagaki *et al.*, 2009), we asked whether the severity of the phenotype may correlate with  
171 the levels of expression for DDR genes. We thus determined the expression level of *BRCA1* that  
172 is involved in the DNA repair and *SMR7* which is an inhibitor of cell cycle progression, in rosette  
173 leaves of *teb* plants. Plants from the two phenotypic classes displayed upregulation both genes as  
174 previously reported (Inagaki *et al.*, 2009), but no significant differences were observed between  
175 *teb* plants with different phenotype (Figure S1).

176 We next asked whether the observed variability in the *teb* mutant phenotype could also be observed  
177 earlier during development. Indeed, when analyzing root length of 15-day-old plants, we observed  
178 that *teb* mutants displayed a higher proportion of plants with arrested root growth than the wild-  
179 type (Figure S2). Likewise, at 10 days after germination, plantlets displayed more variable sizes  
180 than the wild-type, with a higher proportion of small plantlets with shorter roots and smaller  
181 cotyledons (Figure S3A, B). To determine whether this phenotypic variability related to increased  
182 DNA damage accumulation, we performed immuno-labelling of phosphorylated  $\gamma$ -H2AX variant  
183 on root tips of wild-type plants and small and big plantlets of *teb* mutants, that forms foci at the

184 site of DSBs (Charbonnel *et al.*, 2010). As shown on Figure 2, we could observe a significant  
185 increase in  $\gamma$ -H2AX labelling in *teb* mutants: the percentage of root tip nuclei showing  $\gamma$ -H2AX  
186 foci was around 1% in the wild-type, and around 10 % in both *teb* mutant alleles. However, the  
187 percentage of labelled nuclei was not significantly different between big and small plantlets.  
188 Consistently, DDR genes activation did not differ significantly between small and big *teb* mutants  
189 (Figure S3C, D). Furthermore, plants with arrested root growth did not show severe *teb* mutant  
190 plants at later stages: we selected 20 of those plantlets and transferred them to the green house, but  
191 none of them developed a severe phenotype after 3 weeks. Collectively, these results indicate that  
192 loss of Pol  $\theta$  results in an increase in DNA damage accumulation in proliferating cells, but that the  
193 appearance of the *teb* severe phenotype is stochastic, and does not correlate with significantly  
194 higher levels of DNA damage or DDR activation.

195 One possible explanation for the stochastic appearance of the severe phenotype in *teb* mutants  
196 could be the accumulation of mutations as a consequence of defects in DNA repair. Under such a  
197 scenario, developmental defects would be expected to be transmitted to the next generation, or to  
198 aggravate in the next generation. To test this, the progeny of WTL and S plants was sown, and we  
199 evaluated the distribution of plants between the two classes in the next generation. However, the  
200 distribution of plants between the 2 classes was the same in the subsequent generation (Figure S4),  
201 suggesting that developmental defects are not due to mutations.

## 202 **Pol $\theta$ is involved in replicative stress tolerance**

203 Pol  $\theta$  has been proposed to play a key role in replicating cells (Inagaki *et al.*, 2009), we therefore  
204 asked whether replicative stress could increase the proportion of plants showing developmental  
205 defects in *teb* mutants. Wild-type and *teb* mutants were germinated on MS supplemented with  
206 Hydroxyurea (HU, 0.75mM). At 10 days after germination, the survival rate of *teb* mutants was  
207 lower than that of wild-type plants (Figure S5), indicating that *teb* mutants are hypersensitive to  
208 replicative stress. After 10 days, surviving plants were transferred to soil, and the proportion of  
209 plants with a WTL or S phenotype was assessed after 3 weeks. Wild-type (Col-0) plants subjected  
210 to this treatment displayed a growth reduction but did not show other developmental defects such  
211 as deformed leaves (Figure S6). By contrast, as shown on Figure 1E, the proportion of plants with  
212 severe developmental defects was significantly increased in both *teb2* and *teb5* mutants. The

213 proportion of S plants increased from less than 15% to almost 30%, indicating that replicative  
214 stress may be the cause for developmental defects observed in *teb* mutants.

215 To further explore the role Pol  $\theta$  in response to replicative stress, we took advantage of the  
216 hypomorphic mutant *pol2a-4*. This mutant (also called *abo4-1*) is partially deficient for the  
217 replicative DNA polymerase Pol  $\epsilon$  (Yin *et al.*, 2009), and we have shown that it displays  
218 constitutive replicative stress (Pedroza-Garcia *et al.*, 2017). The *teb2* and *teb5* mutations were  
219 therefore introduced in the *pol2a-4* background by crossing, generating the *pol2a teb2* and *pol2a*  
220 *teb5* double mutants.

221 Six weeks old plants of all mutant combinations are shown in Figure 3A. Interestingly, *pol2a teb*  
222 double mutants displayed severe developmental defects that were fully homogeneous between  
223 individuals. To further characterize the developmental defects of *pol2a teb* double mutants, we  
224 quantified root length: we observed that *teb* and *pol2a* roots were shorter compared to wild type  
225 plants, as previously reported (Inagaki *et al.*, 2006; Pedroza-Garcia *et al.*, 2017). In addition, root  
226 length of *pol2a teb* double mutants was significantly reduced compared to single mutants (Figure  
227 3B and 3C). Because *teb* mutants display disorganized meristem and spontaneous cell death in  
228 root tips (Inagaki *et al.*, 2006), we evaluated whether these defects were exacerbated in *pol2a teb*  
229 double mutants. Root tips of eight-day-old plants from mutant combinations were observed by  
230 confocal microscopy after propidium iodide staining. We observed disorganized meristem and cell  
231 death in the *teb* mutants, confirming the result of the previous study (Inagaki *et al.*, 2006).  
232 Furthermore, meristems were severely compromised in *pol2a teb* double mutants (Figure 4A-F)  
233 with disorganized patterning, extensive cell death and differentiation of root hair close to the tip  
234 of the root. Finally, meristem length was measured in these mutants, showing that *pol2a* and *teb*  
235 mutants have smaller root meristem size compared to the wild type Col-0. Moreover, more drastic  
236 reduction of meristem size was observed in the *pol2a teb* double mutants (Figure 4G). Finally,  
237 *pol2a teb* double mutants accumulated significantly higher levels of  $\gamma$ -H2AX foci than *teb* single  
238 mutants, whereas *pol2a* mutants did not accumulate more DSBs than the wild-type, as previously  
239 reported ((Pedroza-Garcia *et al.*, 2017), Figure 2D). Together, these results indicate that cell  
240 proliferation is more severely compromised in *pol2a teb* double mutants than in parental lines,  
241 likely due to increased accumulation of DNA breaks, consistent with the notion that Pol  $\theta$  plays a  
242 key role in the repair of replication-associated DNA damage.

243 Our results indicate that loss of Pol  $\theta$  impairs the repair of replication-associated DNA damage,  
244 which could lead to the activation of the DDR response. To test this hypothesis, we next checked  
245 the expression of DNA damage responsive genes in all mutant combinations by qRT-PCR (Figure  
246 5). We selected genes representative of different responses triggered by DDR activation such as  
247 DNA repair genes (*RAD51* and *BRCA1*) and cell cycle regulation (*SMR5/7*, *WEE1* and *CYCB1*;  
248 1). Expression of all tested genes was induced in the *teb* single mutants and in *pol2a* compared to  
249 wild-type Col-0, consistent with previous reports (Inagaki *et al.*, 2006; Pedroza-Garcia *et al.*,  
250 2017), except for the *WEE1* gene in the *teb5* mutant. Furthermore, these genes displayed an even  
251 higher up-regulation in *pol2a teb* than in the single mutants (Figure 5), indicating that replicative  
252 stress induced by Pol  $\epsilon$  deficiency is enhanced by the lack of Pol  $\theta$ .

### 253 **Abiotic stresses aggravate the severity of *teb* mutants' phenotype.**

254 Taken together, our results indicate that a key cellular function of Pol  $\theta$  is to allow repair of  
255 replication-associated DNA damage. This led us to postulate that the discrepancies between our  
256 observations and previous reports regarding the severity of *teb* mutants' phenotype could stem  
257 from different intensities of basal replicative stress between laboratories, due to different growth  
258 conditions. Under such a scenario, abiotic stresses would be expected to impact the severity of *teb*  
259 mutants' phenotypes. To test this hypothesis, we subjected *teb2* and *teb5* mutants to various abiotic  
260 stress conditions: high light intensity (HL,  $350 \mu\text{mol} \times \text{m}^{-2} \times \text{s}^{-1}$ ), salt treatment (50 or 100 mM of  
261 NaCl). and heat (growth at  $32^{\circ}\text{C}$ ). Except for the HL treatment, plants were grown under a low  
262 light intensity (LL,  $160 \mu\text{mol} \times \text{m}^{-2} \times \text{s}^{-1}$ ). After 3 weeks, we counted the plants in each phenotype  
263 category ( $n > 50$ ). These treatments obviously modified the phenotype of wild-type plants but did  
264 not induce the appearance of the conspicuous *teb*-like phenotype in Col0 plants (Figure S7). It is  
265 worth noting that the HL condition could not be considered as a stress condition for wild-type  
266 plants as they grew faster and reached a larger size than under LL conditions (Figure S7). The  
267 proportion of S plants increased under HL and high salt stress (100mM) for both *teb2* and *teb5*  
268 mutants (Figure 6A, B). By contrast, a lower concentration of salt (50mM) had no impact on the  
269 distribution of *teb* mutants between the different phenotypic classes. Likewise, growth at  $32^{\circ}\text{C}$  did  
270 not significantly affect the proportion of *teb* mutants with a severe phenotype. We tried increasing  
271 the temperature to  $37^{\circ}\text{C}$ , but the proportion of plantlets that did not survive in these growth  
272 conditions was over 50% in both wild-type and mutants, which prevented further analysis. To

273 determine whether abiotic stress conditions affected the level of DDR activation in *teb* mutants,  
274 we monitored the expression of DDR marker genes (Figure S8). Results obtained on mature plants  
275 were too variable to draw robust conclusions, so experiments were performed on *in vitro* grown  
276 plantlets. The two DNA-repair marker genes (*XRI-1* and *BRCA2*) and the cell cycle inhibitor *SMR7*  
277 were induced by salt treatment but not by high-light in wild-type plants, while expression of *SMR5*  
278 did not change between growth conditions. All these genes were induced in *teb2* and *teb5* mutants,  
279 and reached the same levels under control and high-light conditions. By contrast, all tested DDR  
280 marker genes were significantly induced in *teb* mutants grown in the presence of salt compared to  
281 control conditions, although the relative expression compared to wild-type plants remained in the  
282 same range. These results suggest that salt treatment can lead to DDR activation, and that this  
283 phenomenon is amplified in *teb* mutants, consistent with the observation that this treatment leads  
284 to an increase in the proportion of plants with a S phenotype. The situation for high-light response  
285 appears to be less clear, but it is worth noting that *in vitro* growth conditions may not be fully  
286 comparable to growth on soil that we used for plant phenotyping.

287 Together, our results suggest that Pol  $\theta$  is required in proliferating cells for the repair of replication-  
288 induced DNA lesions, and that basal levels of replicative stress vary depending on growth  
289 conditions, which likely accounts for the variability of *teb* mutants' phenotype.

## 290 **DISCUSSION**

291 In mammalian cells, Pol  $\theta$  mediates both error-prone TLS during DNA replication (Yoon *et al.*,  
292 2019; Yousefzadeh and Wood, 2013) and DSB repair through Alt-NHEJ/MMEJ (Beagan and  
293 McVey, 2016). This dual role appears to be conserved in plants. Indeed, previous studies have  
294 shown that plant Pol  $\theta$  is required for plant tolerance to various sources of DNA damage:  
295 *Arabidopsis* *teb* mutants are hypersensitive to damaging agents such as UV, cisplatin, MMC  
296 among others (Inagaki *et al.*, 2006), all of which can induce DNA damage in both proliferating  
297 and differentiated cells. More recently, Pol  $\theta$  was involved in the repair of DSB through Alt-NHEJ  
298 (van Kregten *et al.*, 2016; Nishizawa-Yokoi *et al.*, 2020), a process that may also occur both in  
299 dividing and in differentiated cells. These observations, together with the fact that Pol  $\theta$  appeared  
300 to be required for normal plant development prompted us to ask whether developmental defects  
301 observed in *teb* mutants reflect its function in TLS, DNA repair in all cell types, or repair of



302 replication-associated DNA damage. Here, we were able to show that phenotypic defects triggered  
303 by Pol  $\theta$  deficiency are variable, and that their severity correlates with endogenous replicative  
304 stress levels. Indeed, HU treatment increased the proportion of *teb* mutants displaying severe  
305 developmental defects. Furthermore, DNA Pol  $\epsilon$  deficiency that triggers constitutive replicative  
306 stress via ATR activation (Pedroza-Garcia *et al.*, 2017) abolished the variability of phenotypic  
307 alterations observed in *teb* mutants: *pol2a teb* double mutants all showed the same developmental  
308 defects, including drastically reduced growth, loss of primary root meristem function and extensive  
309 cell death in the root meristem. We therefore conclude that Pol  $\theta$  is required for cellular response  
310 to replicative stress, and that this cellular function accounts for the developmental defects triggered  
311 by Pol  $\theta$  deficiency. This hypothesis is consistent with the observation that *POLQ* genetically  
312 interacts with *ATR* (Inagaki *et al.*, 2009), whose function is to activate the DDR in response to  
313 replicative stress: developmental defects of *teb atr* double mutants are drastically enhanced  
314 compared to *teb* mutants, and inactivation of ATR prevents upregulation of the DDR marker gene  
315 *CYCBI;1* in *teb*. Taken together, these observations indicate that the activity of plant Pol  $\theta$  is  
316 crucial to avoid accumulation of DNA damage during DNA replication in plants. Consistently, in  
317 mammals, the Alt-NHEJ activity is maximal during S-phase (Brambati *et al.*, 2020). Likewise,  
318 mutations in *Drosophila MUS308* gene induce hypersensitivity to replication-blocking lesions  
319 such as inter-strand cross-links (Harris *et al.*, 1996), and Pol  $\theta$  was shown to play a key role in  
320 replication-associated DSB repair (Alexander *et al.*, 2016). A similar finding was reported in  
321 *Caenorhabditis elegans*, where loss of Pol  $\theta$  results in dramatic DNA loss around replication  
322 barriers such as G-quadruplexes (Koole *et al.*, 2014). Thus, repair of DNA breaks generated by  
323 DNA replication appears to be most prominent cellular function of Pol  $\theta$  both in plants and  
324 animals.

325 Another pending question is how essential this replication-associated DNA repair function is for  
326 the normal development of multicellular organisms. The *chaos1* mouse mutants that harbor a point  
327 mutation in the *POLQ* gene are viable but show genomic instability, especially in erythrocytes  
328 (Shima *et al.*, 2004), but otherwise grow normally. *Drosophila* mutants also do not show major  
329 developmental alterations, except for a thin eggshell phenotype (Alexander *et al.*, 2016). In plants,  
330 the situation seems less clear as *Arabidopsis teb* mutants grown under our standard laboratory  
331 conditions display very variable phenotypic defects, and rice mutants grow and develop normally

332 (Nishizawa-Yokoi *et al.*, 2020). Likewise, in the moss *Physcomitrella patens*, loss of Pol  $\theta$  does  
333 not affect development or genetic stability (Mara *et al.*, 2019). The latter observation may relate  
334 to the fact that the most prominent DNA repair pathway in moss cells is homologous  
335 recombination (HR) rather than Alt-NHEJ: in *P. patens*, mutants deficient for the RAD51 protein,  
336 that is required for HR, show developmental defects and hypersensitivity to DNA damaging agents  
337 (Markmann-Mulisch *et al.*, 2007). This suggests that in the moss, replication-associated damage  
338 is repaired mainly by HR rather than via Alt-NHEJ. The existence of alternative repair mechanisms  
339 also likely accounts for the variability observed in *Arabidopsis teb* mutants' phenotypes. HR, or  
340 other back-up repair mechanisms such as canonical NHEJ may compensate for Pol  $\theta$  deficiency  
341 when replicative stress levels are relatively low. However, when the intensity of replicative stress  
342 increases, Pol  $\theta$  becomes indispensable to deal with the accumulating DNA damage, and its  
343 absence leads to cell death and developmental defects. Our working model for Pol  $\theta$  cellular  
344 function is summarized on Figure 7: in the wild-type, Pol  $\theta$  avoids for stalling by promoting TLS,  
345 and contributes to the repair of DSBs generated by the combination of fork collapse and  
346 converging DNA replication coming from a nearby replication origin. Persistent fork stalling or  
347 unrepaired DSBs can activate the DDR via ATR, but this event remains very rare. In the absence  
348 of Pol  $\theta$ , both TLS and DSB repair via Alt-NHEJ are compromised, leading to persistent DNA  
349 damage that activates ATR signaling and the DDR. Interestingly, contrasting requirements for Pol  
350  $\theta$  activity may exist between cell types in higher plants such as *Arabidopsis*. Indeed, Pol  $\theta$  appears  
351 to be strictly required for T-DNA integration when plants are transformed by floral-dip, but not  
352 when transformation is done on somatic cells (Nishizawa-Yokoi *et al.*, 2020). The stochastic  
353 appearance of severe developmental phenotypes in *teb* mutants, and the fact that they are not  
354 heritable through sexual reproduction may be due to the appearance of mutations in somatic cells.  
355 Such a hypothesis would imply that meristematic cells that will give rise to the germline rely on  
356 other DNA repair pathways than Alt-NHEJ, or are more readily eliminated by programmed cell  
357 death than the neighboring initials. A similar situation may exist in animals since in mice, POLQ  
358 deficiency affects genomic stability mainly in erythrocytes (Shima *et al.*, 2004).

359 Requirement for Pol  $\theta$ -dependent DNA repair may differ not only between cell types, but also  
360 between genomic regions. In *Drosophila* follicle cells, replication associated damage is repaired  
361 preferentially by HR or Pol  $\theta$ -dependent Alt-NHEJ depending on the loci (Alexander *et al.*, 2016),

362 suggesting that Pol  $\theta$ -mediated DNA repair is the prevalent DNA repair mechanism after fork  
363 collapse only at a subset of genomic regions. Likewise, in Arabidopsis, the *teb* mutations  
364 specifically affects the expression of genes with a nearby Helitron as well as that of tandem and  
365 dispersed duplicated genes (Inagaki *et al.*, 2009). Authors postulated that the *teb* mutation affects  
366 the chromatin state at these loci due to failed HR. One more likely hypothesis would be that Pol  $\theta$   
367 is preferentially involved in DNA repair at genomic regions that could otherwise engage in  
368 illegitimate HR with duplicated loci to avoid loss of genetic information. In the absence of Pol  $\theta$ ,  
369 DNA repair at these genomic regions would be compromised or delayed, which could indeed  
370 impair the proper re-establishment of chromatin states after DNA replication. This hypothesis  
371 could account for the fact that developmental defects triggered by Pol  $\theta$  vary in severity and are  
372 not transmitted to the next generation through sexual reproduction. Indeed, if developmental  
373 defects associated with Pol  $\theta$  deficiency were due to mutations caused by altered DNA repair, they  
374 would be expected to be stochastic in terms of plants' aspect because mutations could occur  
375 anywhere in the genome, and heritable. On the contrary, the *teb* mutation gives rise to remarkably  
376 similar phenotypical defects that are not heritable, and appear with a variable frequency. Defects  
377 in cell cycle progression very likely contribute to these developmental defects. However, it is  
378 tempting to speculate that they could also partly be due to changes in gene expression triggered by  
379 defects in the restoration of chromatin states after DNA replication. If Pol  $\theta$  is preferentially  
380 involved in DNA repair at specific genomic contexts, this model would also explain why plants  
381 with severe developmental defects all look identical.

382 Finally, our results not only provide evidence for the role of Pol  $\theta$  during DNA replication, but  
383 also reveal that abiotic stresses can enhance the requirement for Pol  $\theta$ , indicating that levels of  
384 replicative stress in dividing cells may differ depending on growth conditions. How abiotic stresses  
385 affect genome integrity in plants remains to be fully elucidated (Nisa *et al.*, 2019). The effect of  
386 UV light or heavy metals on DNA is well documented (Chen *et al.*, 2019), but the consequences  
387 of other stresses such as temperature changes, drought, salinity or light intensity have been less  
388 explored, although there is accumulating evidence that DDR signaling may be a relevant element  
389 in plants' response to these stimuli. Indeed, the ANAC044 and ANAC085 transcription factors,  
390 that are activated by DNA damage also contribute to the induction of a G2-arrest in response to  
391 heat stress (Takahashi *et al.*, 2019). Whether their role reflects the accumulation of DNA damage

392 in response to heat, or the recruitment of this DDR branch to respond to heat stress remains to be  
393 clarified, but these results suggest that DDR signaling may play a more prominent role than  
394 previously anticipated in plants' response to environmental stresses. In line with this hypothesis,  
395 root meristem maintenance under chilling conditions requires DDR signaling components (Hong  
396 *et al.*, 2017). Our results indicate that at least high light and salt may induce replicative stress in  
397 plants, as evidenced by the aggravation of *teb* mutants' phenotypes. By contrast, we could not  
398 detect any effect of heat stress. This may be due to the fact that we exposed plants to a slightly less  
399 severe heat stress than Takahashi and colleagues (Takahashi *et al.*, 2019) because prolonged  
400 growth at 37°C resulted in a high mortality rate in both wild-type and mutant plants. However, this  
401 could also mean that all types of abiotic stresses do not affect DNA replication in the same way.  
402 Future work should help elucidate how much mechanisms involved in the maintenance of genome  
403 integrity contribute to plants developmental plasticity in response to stress, and whether different  
404 stress conditions affect genome integrity in different ways.

405

## 406 MATERIAL AND METHODS

### 407 Plant material and growth conditions

408 All *Arabidopsis thaliana* mutants used in this study are in the wild type Columbia-0 (Col-0)  
409 background. *teb2* (SALK\_035610) and *teb5* (SALK\_018851) mutants were a kind gift from M.  
410 van Kregten (Leiden University).

411 Seeds were surface sterilized and treated with bayrochlore™ for 20 min, then washed with sterile  
412 water and kept at 4°C for 2 days. They were next sown on commercially available 0.5× Murashige  
413 and Skoog (MS, Duchefa) medium solidified with 0.8% agar (Phyto-Agar HP696, Kalys). Plates  
414 were then transferred to a long day (16 h light, 8 h night, 21°C) *in vitro* growth chamber. After 2  
415 weeks plants were transferred to soil under short day conditions (8 h light 20°C, 16 h night at 18°C)  
416 for one week and after that transferred to a long day growth chamber (16 h light, 8 h night, 21°C)  
417 for phenotypic analysis.

418 Genotyping of the *teb2* and *teb5* mutants was performed using the Lba1/RP primer combination  
419 for the mutant allele and the LP/RP primer combination for the wild-type allele. Sequence of  
420 primers used can be found in Table S1.

#### 421 **Genotoxic test**

422 Wild type Col-0 and *teb* mutants *teb2* and *teb5*) were germinated on MS medium (Control  
423 condition) and some were germinated on MS supplemented hydroxyurea (HU) concentration was  
424 0.75 mM. After 2 weeks, these mutant plants were transferred to soil. Then after 10 days, the  
425 survival rate of these plants was measured.

#### 426 **RNA extraction and quantitative RT-PCR**

427 Total RNA was extracted from flower buds using NucleoSpin® RNA protocol (MACHEREY-  
428 NAGEL). First strand cDNA was synthesized from 2µg of total RNAs by using ImProm-II™  
429 Reverse Transcription System (Promega) according to the manufacturer's instructions. 1/50<sup>th</sup> of  
430 the synthesized cDNA was mixed with 100nM of each primer and LightCycler 480 Sybr Green I  
431 mastermix (Roche Applied Science) for quantitative PCR analysis. Products were amplified and  
432 fluorescent signals acquired with a LightCycler 480 detection system. The specificity of  
433 amplification products was determined by melting curves. Data were from triplicates and are  
434 representative of at least two biological replicates. The sequence of primers used in this study is  
435 provided in Supplementary Table 1. DDR-related genes expressions were normalized by using  
436 housekeeping gene *ACTIN*. Similar results were observed in 3 independent experiments.

437

#### 438 **Immuno-fluorescence**

439 Immuno-labelling of  $\gamma$ -H2AX foci was performed as described previously (Charbonnel *et al.*,  
440 2010). Slides were imaged with an epifluorescence microscope (AxioImager Z.2; Carl Zeiss) fitted  
441 with a metal halide lamp and the appropriate shifted free filter sets for imaging DAPI and Alexa  
442 488 dyes. Images were acquired with a cooled CCD camera (AxioCam 506 monochrome; Carl  
443 Zeiss) operated using Zen Blue software (Carl Zeiss).

444

#### 445 **Confocal microscopy imaging**

446 Root tips of 8-day-old plantlets were stained with propidium iodide (PI, 10 $\mu$ M) and then root  
447 meristems were observed using 20X water immersion lens on a Zeiss LSM 880 laser scanning  
448 confocal microscope using a 561nm laser for excitation. Fluorescence was acquired between 565  
449 nm and 700 nm. Representative images were collected from 10 to 15 roots with three biological  
450 replicates.

#### 451 **Abiotic stress**

452 In this study three different abiotic stress were applied on *teb* mutants. These mutant seeds were  
453 grown on 1/2 MS medium and germinated *in vitro* and after 10 days transferred to pots (soil).  
454 Control plants were kept at 20°C under low light intensity (LL, 160 $\mu$ mol x m<sup>-2</sup> x s<sup>-1</sup>), and watered  
455 with water. Plants were either subjected to high light intensity (HL, 350  $\mu$ mol x m<sup>-2</sup> x s<sup>-1</sup>) at 20°C,  
456 or transferred in a growth cabinet at 32°C (16h day, 8h night, 28°C at night) under LL or kept at  
457 20°C under LL but watered with two NaCl solutions (50mM or 100mM). For the higher salt  
458 concentration, plants were first watered with NaCl for 3 days, and the concentration was then  
459 increased to 100mM. Distribution of plants between the three phenotypic classes was documented  
460 after three weeks of these stresses. Chi-squared tests was used to compare the distributions between  
461 phenotypic classes. Experiments were performed twice giving similar results.

#### 462 **Accession numbers**

463 Accession numbers of the genes mentioned in this study are as follows: *TEBICHI* (AT4G32700),  
464 *POL2A* (AT1G08260), *CYCB1;1* (AT4G37490), *RAD51* (AT5G20850), *WEE1* (AT1G02970),  
465 *BRCA2* (AT1G80210), *SMR5* (AT1G07500), *SMR7* (AT3G27630).

#### 466 **Acknowledgements**

467 Maherun Nisa is supported by a grant from the Fondation pour la Recherche Médicale  
468 (ECO201806006824). We thank Marleen van Kregten for providing the seeds of the *teb* mutants  
469 and Charles White (GReD, Clermont-Ferrand) for the kind gift of the anti  $\gamma$ -H2AX antibody. We  
470 thank Maxence Remerand and Lazare Brezillon-Dubus, who helped characterizing *pol2a teb*  
471 double mutants during their internship. The present work has benefited from the core imaging  
472 facilities of IPS2 supported by the Labex ‘Saclay PlantScience’ (ANR-11-IDEX-0003-02).

#### 473 **Conflict of interest**

474 Authors declare no conflict of interest.

475

## 476 REFERENCES

477 **Adachi, S., Minamisawa, K., Okushima, Y., et al.** (2011) Programmed induction of  
478 endoreduplication by DNA double-strand breaks in Arabidopsis. *Proc Natl Acad Sci U S A*,  
479 **108**, 10004–10009. Available at: <http://www.ncbi.nlm.nih.gov/pubmed/21613568>.

480 **Alexander, J.L., Beagan, K., Orr-Weaver, T.L. and McVey, M.** (2016) Multiple mechanisms  
481 contribute to double-strand break repair at rereplication forks in Drosophila follicle cells.  
482 *Proc. Natl. Acad. Sci. U. S. A.*, **113**, 13809–13814. Available at:  
483 <http://www.ncbi.nlm.nih.gov/pubmed/27849606> [Accessed June 17, 2020].

484 **Beagan, K. and McVey, M.** (2016) Linking DNA polymerase theta structure and function in  
485 health and disease. *Cell. Mol. Life Sci.*, **73**, 603–15. Available at:  
486 <http://www.ncbi.nlm.nih.gov/pubmed/26514729> [Accessed June 16, 2020].

487 **Brambati, A., Barry, R.M. and Sfeir, A.** (2020) DNA polymerase theta (Polu)-an error-prone  
488 polymerase necessary for genome stability. *Curr Opin Genet Dev*, **60**, 119–126. Available  
489 at: <https://doi.org/10.1016/j.gde.2020.02.017>.

490 **Burgers, P.M.J.** (1998) Eukaryotic DNA polymerases in DNA replication and DNA repair.  
491 *Chromosoma*.

492 **Charbonnel, C., Gallego, M.E. and White, C.I.** (2010) Xrcc1-dependent and Ku-dependent  
493 DNA double-strand break repair kinetics in Arabidopsis plants. *Plant J.*, **64**, 280–290.  
494 Available at: <http://www.ncbi.nlm.nih.gov/pubmed/21070408> [Accessed October 14, 2015].

495 **Chen, P., Sjogren, C.A., Larsen, P.B. and Schnittger, A.** (2019) A multi-level level response  
496 to DNA damage induced by Aluminium. *Plant J.*, **98**, 479-491.

497 **Chiruvella, K.K., Liang, Z. and Wilson, T.E.** (2013) Repair of double-strand breaks by end  
498 joining. *Cold Spring Harb. Perspect. Biol.*, **5**, a012757. Available at:  
499 <http://www.ncbi.nlm.nih.gov/pubmed/23637284> [Accessed June 16, 2020].

500 **Ciccia, A. and Elledge, S.J.** (2010) The DNA Damage Response: Making It Safe to Play with  
501 Knives. *Mol. Cell*.

502 **Feng, W., Simpson, D.A., Carvajal-Garcia, J., et al.** (2019) Genetic determinants of cellular  
503 addiction to DNA polymerase theta. *Nat. Commun.*, **10**, 1–13. Available at:  
504 <https://doi.org/10.1038/s41467-019-12234-1> [Accessed October 26, 2020].

505 **Fulcher, N. and Sablowski, R.** (2009) Hypersensitivity to DNA damage in plant stem cell  
506 niches. *Proc Natl Acad Sci U S A*, **106**, 20984–20988. Available at:  
507 [http://www.ncbi.nlm.nih.gov/entrez/query.fcgi?cmd=Retrieve&db=PubMed&dopt=Citation](http://www.ncbi.nlm.nih.gov/entrez/query.fcgi?cmd=Retrieve&db=PubMed&dopt=Citation&list_uids=19933334)  
508  [&list\\_uids=19933334](http://www.ncbi.nlm.nih.gov/entrez/query.fcgi?cmd=Retrieve&db=PubMed&dopt=Citation&list_uids=19933334).

509 **Harris, P. V, Mazina, O.M., Leonhardt, E.A., Case, R.B., Boyd, J.B. and Burtis, K.C.**  
510 (1996) Molecular cloning of Drosophila mus308, a gene involved in DNA cross-link repair  
511 with homology to prokaryotic DNA polymerase I genes. *Mol. Cell. Biol*.

512 **Hong, J.H., Savina, M., Du, J., Devendran, A., Kannivadi Ramakanth, K., Tian, X., Sim,**  
513 **W.S., Mironova, V. V. and Xu, J.** (2017) A Sacrifice-for-Survival Mechanism Protects  
514 Root Stem Cell Niche from Chilling Stress. *Cell*, **170**, 102-113.e14. Available at:  
515 <http://www.ncbi.nlm.nih.gov/pubmed/28648662> [Accessed November 18, 2018].

516 **Hu, Z., Cools, T. and Veylder, L. De** (2016) Mechanisms Used by Plants to Cope with DNA  
517 Damage. *Annu. Rev. Plant Biol.*, **67**, 439–62. Available at:  
518 <http://www.ncbi.nlm.nih.gov/pubmed/26653616> [Accessed July 14, 2016].

519 **Inagaki, S., Nakamura, K. and Morikami, A.** (2009) A link among DNA replication,  
520 recombination, and gene expression revealed by genetic and genomic analysis of TEBICHI  
521 gene of Arabidopsis thaliana P. S. Schnable, ed. *PLoS Genet*, **5**, e1000613. Available at:  
522 <https://dx.plos.org/10.1371/journal.pgen.1000613> [Accessed July 30, 2019].

523 **Inagaki, S., Suzuki, T., Ohto, M., Urawa, H., Horiuchi, T., Nakamura, K. and Morikami,**  
524 **A.** (2006) Arabidopsis TEBICHI, with helicase and DNA polymerase domains, is required  
525 for regulated cell division and differentiation in meristems. *Plant Cell*, **18**, 879–92.  
526 Available at: <http://www.ncbi.nlm.nih.gov/pubmed/16517762> [Accessed July 30, 2019].



527 **Jain, R., Aggarwal, A.K. and Rechkoblit, O.** (2018) Eukaryotic DNA polymerases. *Curr.*  
528 *Opin. Struct. Biol.*, **53**, 77–87. Available at:  
529 <http://www.ncbi.nlm.nih.gov/pubmed/30005324> [Accessed February 12, 2019].

530 **Koole, W., Schendel, R. Van, Karambelas, A.E., Heteren, J.T. Van, Okihara, K.L. and**  
531 **Tijsterman, M.** (2014) A polymerase theta-dependent repair pathway suppresses extensive  
532 genomic instability at endogenous G4 DNA sites. *Nat. Commun.*, **5**. Available at:  
533 <https://pubmed.ncbi.nlm.nih.gov/24496117/> [Accessed October 31, 2020].

534 **Kregten, M. van, Pater, S. de, Romeijn, R., Schendel, R. van, Hooykaas, P.J.J. and**  
535 **Tijsterman, M.** (2016) T-DNA integration in plants results from polymerase- $\theta$ -mediated  
536 DNA repair. *Nat. Plants*, **2**, 16164. Available at:  
537 <http://www.nature.com/articles/nplants2016164> [Accessed July 30, 2019].

538 **Kunkel, T.A.** (2004) DNA replication fidelity. *J. Biol. Chem.*, **279**, 16895–8. Available at:  
539 <http://www.ncbi.nlm.nih.gov/pubmed/14988392> [Accessed February 12, 2019].

540 **Makarova, K.S. and Koonin, E. V** (2013) Archaeology of eukaryotic DNA replication. *Cold*  
541 *Spring Harb. Perspect. Biol.*, **5**, a012963. Available at:  
542 <http://cshperspectives.cshlp.org/lookup/doi/10.1101/cshperspect.a012963> [Accessed  
543 September 9, 2019].

544 **Mara, K., Charlot, F., Guyon-Debast, A., Schaefer, D.G., Collonnier, C., Grelon, M. and**  
545 **Nogu e, F.** (2019) POLQ plays a key role in the repair of CRISPR/Cas9-induced double-  
546 stranded breaks in the moss *Physcomitrella patens*. *New Phytol.*

547 **Markmann-Mulisch, U., Wendeler, E., Zobell, O., Schween, G., Steinbiss, H.H. and Reiss,**  
548 **B.** (2007) Differential requirements for RAD51 in *Physcomitrella patens* and *Arabidopsis*  
549 *thaliana* development and DNA damage repair. *Plant Cell*, **19**, 3080–3089. Available at:  
550 <https://pubmed.ncbi.nlm.nih.gov/17921313/> [Accessed October 31, 2020].

551 **Mateos-Gomez, P.A., Kent, T., Deng, S.K., McDevitt, S., Kashkina, E., Hoang, T.M.,**  
552 **Pomerantz, R.T. and Sfeir, A.** (2017) The helicase domain of Pol $\theta$  counteracts RPA to  
553 promote alt-NHEJ. *Nat. Struct. Mol. Biol.*, **24**, 1116–1123. Available at:  
554 <http://www.ncbi.nlm.nih.gov/pubmed/29058711> [Accessed June 16, 2020].

555 **Nisa, M.-U., Huang, Y., Benhamed, M. and Raynaud, C.** (2019) The Plant DNA Damage  
556 Response: Signaling Pathways Leading to Growth Inhibition and Putative Role in Response  
557 to Stress Conditions. *Front. Plant Sci.*, **10**, 653. Available at:  
558 <http://www.ncbi.nlm.nih.gov/pubmed/31164899> [Accessed July 28, 2019].

559 **Nishizawa-Yokoi, A., Saika, H., Hara, N., Lee, L., Toki, S. and Gelvin, S.B.** (2020)  
560 *Agrobacterium* T-DNA integration in somatic cells does not require the activity of DNA  
561 polymerase theta. *New Phytol.*, nph.17032. Available at:  
562 <https://onlinelibrary.wiley.com/doi/10.1111/nph.17032> [Accessed October 31, 2020].

563 **Noctor, G. and Foyer, C.H.H.** (2016) Intracellular Redox Compartmentation and ROS-Related  
564 Communication in Regulation and Signaling. *Plant Physiol.*, **171**, 1581–92. Available at:  
565 <http://www.ncbi.nlm.nih.gov/pubmed/27208308> [Accessed March 6, 2019].

566 **Pedroza-Garcia, J.-A., Veylder, L. De and Raynaud, C.** (2019) Plant DNA Polymerases. *Int.*  
567 *J. Mol. Sci.*, **20**. Available at: <http://www.ncbi.nlm.nih.gov/pubmed/31569730> [Accessed  
568 June 16, 2020].

569 **Pedroza-Garcia, J.A., Mazubert, C., Olmo, I. Del, et al.** (2017) Function of the plant DNA  
570 Polymerase epsilon in replicative stress sensing, a genetic analysis. *Plant Physiol.*, **173**,  
571 1735-1749.

572 **Powers, K.T. and Washington, M.T.** (2018) Eukaryotic translesion synthesis: Choosing the  
573 right tool for the job. *DNA Repair (Amst.)*, **71**, 127–134. Available at:  
574 <https://www.sciencedirect.com/science/article/pii/S1568786418301812?via%3Dihub>  
575 [Accessed February 12, 2019].

576 **Sakamoto, A.N.** (2019) Translesion Synthesis in Plants: Ultraviolet Resistance and Beyond.  
577 *Front. Plant Sci.*, **10**, 1208. Available at: [www.frontiersin.org](http://www.frontiersin.org) [Accessed November 18,  
578 2020].

579 **Shima, N., Munroe, R.J. and Schimenti, J.C.** (2004) The mouse genomic instability mutation  
580 chaos1 is an allele of Polq that exhibits genetic interaction with Atm. *Mol. Cell. Biol.*, **24**,  
581 10381–9. Available at: <http://www.ncbi.nlm.nih.gov/pubmed/15542845> [Accessed June 17,  
582 2020].

583 **Takahashi, N., Ogita, N., Takahashi, T., Taniguchi, S., Tanaka, M., Seki, M. and Umeda,**  
584 **M.** (2019) A regulatory module controlling stress-induced cell cycle arrest in Arabidopsis.  
585 *Elife*, **8**. Available at: <http://www.ncbi.nlm.nih.gov/pubmed/30944065> [Accessed April 24,  
586 2019].

587 **Wang, Z., Song, Y., Li, S., Kurian, S., Xiang, R., Chiba, T. and Wu, X.** (2019) DNA  
588 polymerase (POLQ) is important for repair of DNA double-strand breaks caused by fork  
589 collapse. *J. Biol. Chem.*, **294**, 3909–3919. Available at:  
590 </pmc/articles/PMC6422074/?report=abstract> [Accessed October 31, 2020].

591 **Yang, W. and Gao, Y.** (2018) Translesion and Repair DNA Polymerases: Diverse Structure and  
592 Mechanism. *Annu. Rev. Biochem.*, **87**, 239–261. Available at:  
593 <https://www.annualreviews.org/doi/10.1146/annurev-biochem-062917-012405> [Accessed  
594 September 9, 2019].

595 **Yin, H., Zhang, X., Liu, J., Wang, Y., He, J., Yang, T., Hong, X., Yang, Q. and Gong, Z.**  
596 (2009) Epigenetic regulation, somatic homologous recombination, and abscisic acid  
597 signaling are influenced by DNA polymerase epsilon mutation in Arabidopsis. *Plant Cell*,  
598 **21**, 386–402. Available at: <http://www.ncbi.nlm.nih.gov/pubmed/19244142>.

599 **Yoon, J.-H., McArthur, M.J., Park, J., Basu, D., Wakamiya, M., Prakash, L. and Prakash,**  
600 **S.** (2019) Error-Prone Replication through UV Lesions by DNA Polymerase  $\theta$  Protects  
601 against Skin Cancers. *Cell*, **176**, 1295-1309.e15. Available at:  
602 <http://www.ncbi.nlm.nih.gov/pubmed/30773314> [Accessed June 17, 2020].

603 **Yoshiyama, K.O., Kobayashi, J., Ogita, N., Ueda, M., Kimura, S., Maki, H. and Umeda, M.**  
604 (2013) ATM-mediated phosphorylation of SOG1 is essential for the DNA damage response  
605 in Arabidopsis. *EMBO Rep*, **14**, 817–822. Available at:  
606 <http://www.ncbi.nlm.nih.gov/pubmed/23907539>.

607 **Yousefzadeh, M.J. and Wood, R.D.** (2013) DNA polymerase POLQ and cellular defense  
608 against DNA damage. *DNA Repair (Amst.)*, **12**, 1–9. Available at:  
609 </pmc/articles/PMC3534860/?report=abstract> [Accessed November 18, 2020].

610 **Zeman, M.K. and Cimprich, K.A.** (2014) Causes and consequences of replication stress. *Nat.*

612

## 613 **Figure Legends**

### 614 **Figure 1: The *tebichi* mutation results in variable developmental defects that can be enhanced** 615 **by replicative stress**

616 A: Representative phenotypes observed in *teb-2* and *teb-5* homozygous mutants after 1 month of  
617 growth on soil. Plants were classified in 3 categories: wild-type like (WT), intermediate (I) with  
618 only mild growth reduction and a few deformed or twisted leaves (arrowhead), or severe (S) with  
619 clear growth reduction and abnormal leaf shape. Bar = 1cm.

620 B: Structure of the *POLQ* gene and position of the T-DNA insertions in the *teb2* and *teb5* alleles.  
621 Exons are indicated by grey boxes and introns by a grey line. Primers used for genotyping are  
622 indicated by arrows.

623 C: Result of genotyping for *teb* mutants with wild-type-like (WTL) or severe (S) phenotype. Both  
624 types of plants were found to be homozygous for the *teb* mutation.

625 D: qPCR quantification of *POLQ* expression in *teb* mutants. Actin was used for normalization.  
626 The position of primer pairs is indicated by corresponding numbers.

627 E: Distribution of *teb* mutants between the three phenotypic classes with and without HU  
628 treatment. Plants were germinated on control (MS) or hydroxyurea supplemented medium (HU)  
629 to a final concentration of 0.75mM. They were transferred to soil after 12 days, and phenotypes  
630 were observed after one month. Asterisks denote significant differences between distributions  
631 (Chi-squared test,  $p < 0.01$ ). Blind scoring was performed on wild-type and *teb* mutants, the  
632 proportion of severe phenotypes observed in wild-type plants was below 2% in all conditions.

633

### 634 **Figure 2: *teb* mutants show DSB accumulation in root meristems**

635 A-C: representative images of *teb2* root tip nuclei after g-H2AX immuno-staining (A: DAPI  
636 fluorescence, B: Alexa 488 fluorescence, C: merged image). Bar = 10 $\mu$ m, arrows indicate nuclei  
637 with g-H2AX foci. D: quantification of  $\gamma$ -H2AX foci in the indicated genotypes ( $n > 1500$  nuclei  
638 imaged from 10 root tips for all genotypes). Different letters indicate statistically different values,

639 ANOVA followed by a post-hoc Tukey test  $p < 0.01$ ). Data are representative of 2 biological  
640 replicates.

641

642 **Figure 3: Constitutive replicative stress aggravates the phenotype of *teb* mutants**

643 A: Phenotype of the wild-type (Col0), *teb-2*, *teb-5*, *pol2a-4*, *pol2a teb2* and *pol2a teb5* mutants  
644 after 40 days of growth under standard conditions ( $160 \mu\text{mol photon} \times \text{m}^{-2}\text{xs}^{-1}$ , 16h light,  $20^\circ\text{C}$ ).  
645 Bar = 1cm.

646 B: Root length of the wild-type (Col0), *teb-2*, *teb-5*, *pol2a-4*, *pol2a teb2* and *pol2a teb5*. Plants  
647 were grown vertically *in vitro* for one week.

648 C: Quantification of the root length in the different genotypes. Data are from at least 20  
649 measurements for each line and are representative of 2 independent experiments. Different letters  
650 indicate statistically significant differences (ANOVA and Tukey test  $p < 0.01$ ).

651

652 **Figure 4: The root meristem of *teb pol2a* double mutants is severely compromised**

653 A-F: Confocal images of root tips of 8-day-old plants stained with propidium iodide. A: WT  
654 (Col0), B: *teb2*, C: *teb5*, D: *pol2a-4*, E: *pol2a teb2* F: *pol2a teb5*. The meristem of *teb* mutants  
655 showed abnormal organization and cell death. This defect was exacerbated in *pol2a teb* double  
656 mutants with root hair differentiating close to the root tip and meristem organization being  
657 dramatically altered. Red arrow indicates the limit of the root apical meristem. Bar =  $50\mu\text{m}$  for all  
658 panels.

659 G: Meristem length was measured in all mutant combinations. Values are from at least 10 roots  
660 and are representative of two independent experiments. Different letters indicate statistically  
661 significant differences (ANOVA and Tukey test  $p < 0.01$ ).

662

663 **Figure 5: DDR genes are hyper-induced in *teb pol2a* double mutants**

664 Total RNA was extracted from twelve-day-old plantlets. Expression of selected genes was  
665 assessed by real-time qPCR and normalized to actin. We monitored the expressions of genes  
666 involved in cell-cycle arrest (*SMR5*, *SMR7* and *WEE1*), DNA repair (*RAD51* and *BRCA2*) and both  
667 (*CYCB1;1*). Values are Fold change compared to the wild-type Col-0. Graphs represent average  
668 of 3 technical replicates +/- standard deviation and are representative of 3 independent biological

669 replicates. Different letters above bars denote statistically relevant differences (ANOVA followed  
670 by Tukey test, performed on raw data before normalization,  $p < 0.01$ ).

671

672 **Figure 6: Some abiotic stresses aggravate the developmental defects of *teb* mutants.**

673 A: Distribution of *teb* mutants between the different classes in plants grown in low light (LL,  
674  $160\mu\text{mol} \times \text{m}^{-2} \times \text{s}^{-1}$ ) or high light (HL,  $350\mu\text{mol} \times \text{m}^{-2} \times \text{s}^{-1}$ ).

675 B: Distribution of *teb* mutants between the different classes in plants grown at standard  
676 temperature ( $20^\circ\text{C}$ ) or under heat stress ( $32^\circ\text{C}$ ). Plants were germinated *in vitro* and transferred to  
677 soil after 10 days. After 3 days of growth under control conditions at  $160\mu\text{mol} \times \text{m}^{-2} \times \text{s}^{-1}$  plants  
678 were kept under the same conditions or transferred to  $32^\circ\text{C}$  under the same light intensity.

679 C: Distribution of *teb* mutants between the different classes in plants watered with or without salt  
680 to the indicated concentration. Plants were germinated *in vitro* and transferred to soil after 10 days.  
681 After 3 days of growth under control conditions ( $160\mu\text{mol} \times \text{m}^{-2} \times \text{s}^{-1}$ ,  $20^\circ\text{C}$ , salt-treated plants  
682 were watered with a solution containing NaCl (50mM), for the 100mM treatment, salt  
683 concentration was increased to 100mM after 2days.

684 For all panels, n.s. indicates non-significant differences and asterisks denote significant  
685 differences between distributions (Chi-squared test,  $p < 0.01$ ). Blind scoring was performed on wild-  
686 type and *teb* mutants in all growth conditions, the proportion of severe phenotypes observed in wild-  
687 type plants was below 2%.

688

689 **Figure 7: Model for the role of Pol  $\theta$  during replicative stress response**

690 A: In the wild-type, replication blocking lesions induce fork stalling. Pol  $\theta$  can allow TLS through  
691 some lesions such as pyrimidine dimers. If efficient lesion bypass cannot be achieved, replisome  
692 disassembly and persistent fork stalling activates the DDR through ATR signalling, and DNA  
693 synthesis from a converging fork can lead to the formation of a double-ended DSB. Pol  $\theta$   
694 contributes to the repair of these lesions through Alt-NHEJ but other pathways such as HR or  
695 NHEJ likely contribute to DSB repair. B: In the absence of Pol  $\theta$ , TLS through some lesions is  
696 compromised, leading to an increased frequency of fork collapse and persistent stalling.  
697 Furthermore, Alt-NHEJ is also compromised; leading to an increased frequency of failed repair,  
698 constitutive activation of the DDR through ATR signalling, cell death and stochastic

699 developmental defects. Abiotic stress and replicative stress can modify this equilibrium by  
700 enhancing the accumulation of more replication-blocking lesions, leading to an increased  
701 frequency of developmental defects in Pol  $\theta$  deficient lines.

702

### 703 **Supplemental Figures**

704 **Figure S1: Levels of DDR genes induction do not correlate with the severity of *teb* mutants’**  
705 **phenotype.**

706 **Figure S2: Root growth defects show some heterogeneity in *teb* mutants**

707 **Figure S3: Heterogeneous phenotypes of *teb* mutant plantlets do not correlate with different**  
708 **levels of DDR genes activation**

709 **Figure S4: The *teb* phenotype does not aggravate over generations**

710 **Figure S5: *teb* mutants are hypersensitive to replicative stress**

711 **Figure S6: Representation phenotypes of wild-type (Col0) and *teb* mutants exposed to HU**  
712 **before transfer to the green house**

713 **Figure S7: Representation phenotypes of wild-type (Col0) and *teb* mutants grown under**  
714 **different conditions.**

715 **Figure S8: Salt treatment, but not increasing light intensity activates DDR gene expression**  
716 **in both wild-type and *teb* mutants.**

717

718

### 719 **Supplemental Tables**

720 **Table S1: Primer sequences**

721

722

723

724

725

726

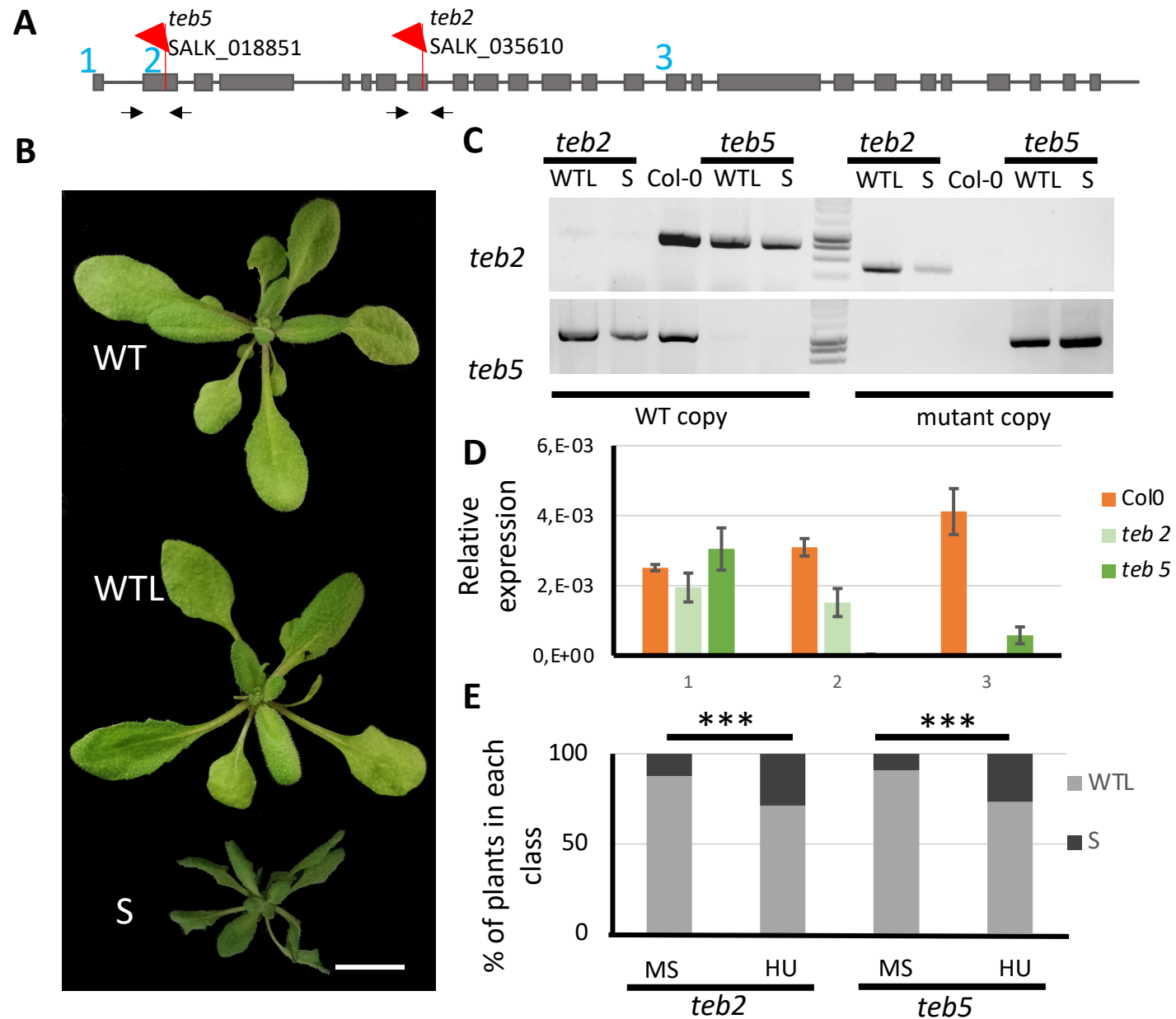


**Figure 1. The *tebichi* mutation results in variable developmental defects that can be enhanced by replicative stress**

**A:** Structure of the *POLQ* gene and position of the T-DNA insertions in the *teb2* and *teb5* alleles. Exons are indicated by grey boxes and introns by a grey line. Primers used for genotyping are indicated by arrows. **B:** Representative phenotypes observed in *teb-2* and *teb-5* homozygous mutants after 1 month of growth on soil. Plants were classified in 2 categories: wild-type like (WTL) and severe (S) with clear growth reduction and abnormal leaf shape. Bar = 1cm. **C:** Result of genotyping for *teb* mutants with wild-type-like (WTL) or severe (S) phenotype. Both types of plants were found to be homozygous for the *teb* mutation. **D:** qPCR quantification of *POLQ* expression in *teb* mutants. Actin was used for normalization. The position of primer pairs is indicated by corresponding numbers in (A). Data are average  $\pm$  S.D. of three technical replicates and representative of three independent experiments. **E:** Distribution of *teb* mutants between the two phenotypic classes with and without HU treatment. Plants were germinated on control (MS) or hydroxyurea supplemented medium (HU) to a final concentration of 0.75 mM. They were transferred to soil after 12 days, and phenotypes were observed after one month ( $n > 50$ ). Asterisks denote statistically relevant differences between distributions ( $\chi^2$ -test,  $p < 0.01$ ). Blind scoring was performed on wild-type and *teb* mutants, the proportion of severe phenotypes observed in wild-type plants was below 2% in all conditions.



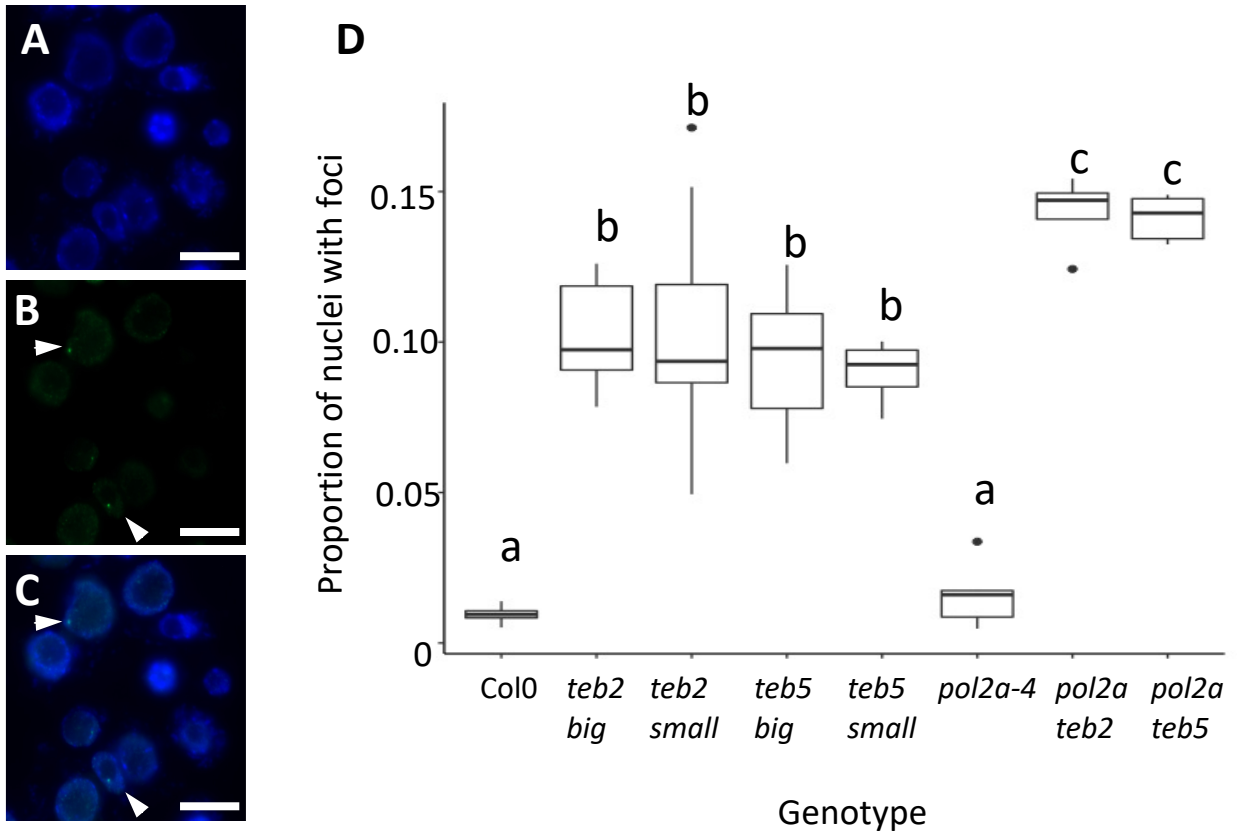


**Figure 2. *teb* mutants show DSB accumulation in root meristems**

A-C: representative images of *teb2* root tip nuclei after  $\gamma$ -H2AX immuno-staining (A: DAPI fluorescence, B: Alexa 488 fluorescence, C: merged image). Bar = 10  $\mu$ m, arrows indicate nuclei with  $\gamma$ -H2AX foci. D: quantification of  $\gamma$ -H2AX foci in the indicated genotypes ( $n > 1500$  nuclei imaged from 10 root tips for all genotypes). Different letters indicate statistically different values, ANOVA followed by a post-hoc Tukey test  $p < 0.01$ ). Data are representative of 2 biological replicates.

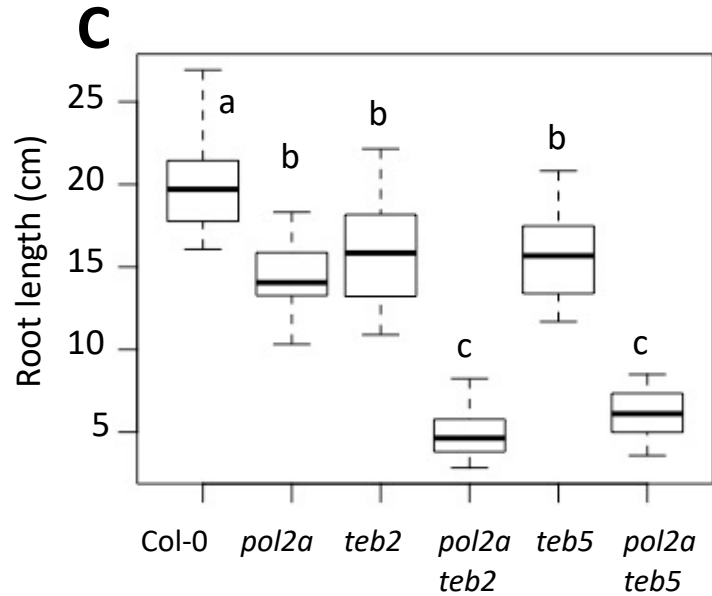
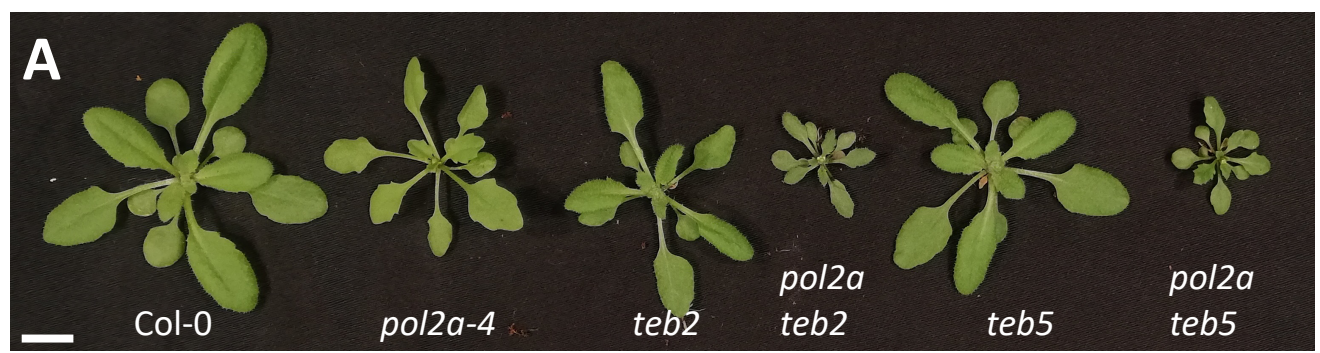


**Figure 3. Constitutive replicative stress aggravates the phenotype of *teb* mutants**

A: Phenotype of the wild-type (Col0), *teb-2*, *teb-5*, *pol2a-4*, *pol2a teb2* and *pol2a teb5* mutants after 40 days of growth under standard conditions ( $160 \mu\text{mol photon} \times \text{m}^{-2}\text{xs}^{-1}$ , 16h light,  $20^\circ\text{C}$ ). Bar = 1 cm.

B: Root length of the wild-type (Col0), *teb-2*, *teb-5*, *pol2a-4*, *pol2a teb2* and *pol2a teb5*. Plants were grown vertically *in vitro* for one week.

C: Quantification of the root length in the different genotypes. Data are from at least 20 measurements for each line and are representative of 2 independent experiments. Different letters indicate statistically relevant differences (ANOVA and Tukey test  $p < 0.01$ ).

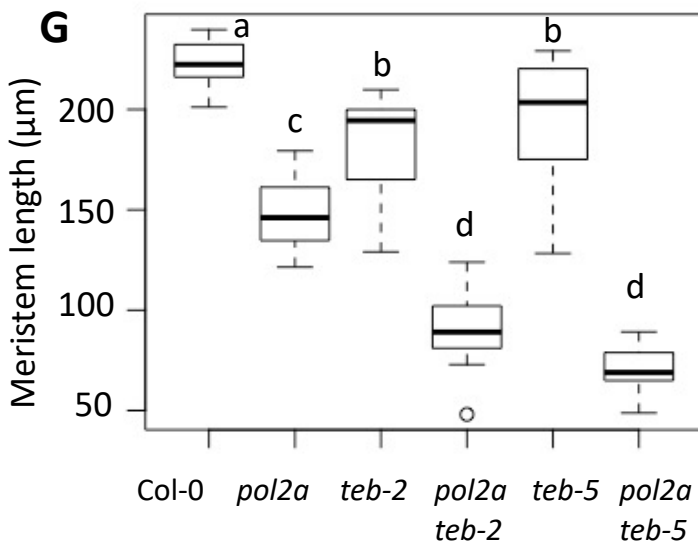
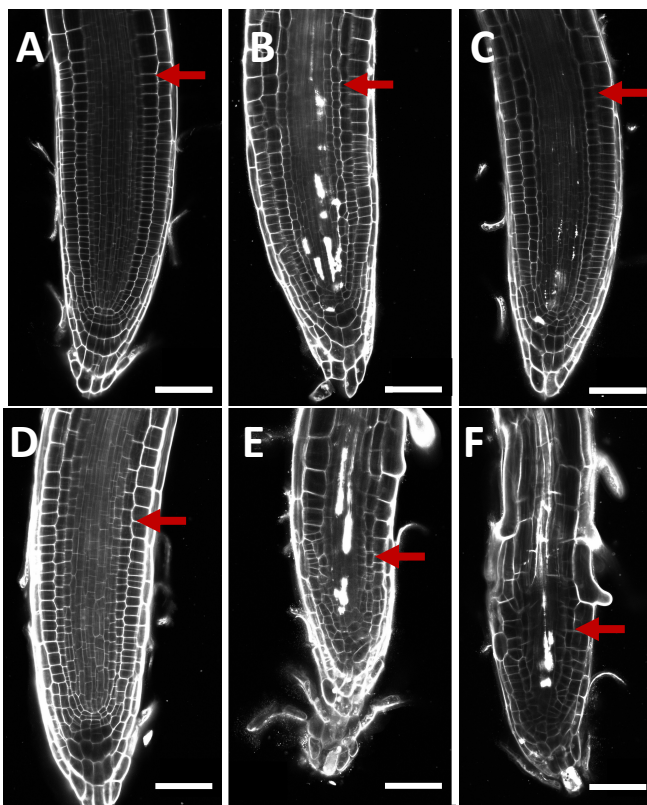


**Figure 4. The root meristem of *teb pol2a* double mutants is severely compromised**

A-F: Confocal images of root tips of 8-day-old plants stained with propidium iodide. A: WT (Col0), B: *teb2*, C: *teb5*, D: *pol2a-4*, E: *pol2a teb2* F: *pol2a teb5*. The meristem of *teb* mutants showed abnormal organization and cell death. This defect was exacerbated in *pol2a teb* double mutants with root hair differentiating close to the root tip and meristem organization being dramatically altered. Red arrow indicates the limit of the root apical meristem. Bar = 50  $\mu$ m for all panels.

G: Meristem length was measured in all mutant combinations. Values are from at least 10 roots and are representative of two independent experiments. Different letters indicate statistically relevant differences (ANOVA and Tukey test  $p < 0.01$ ).

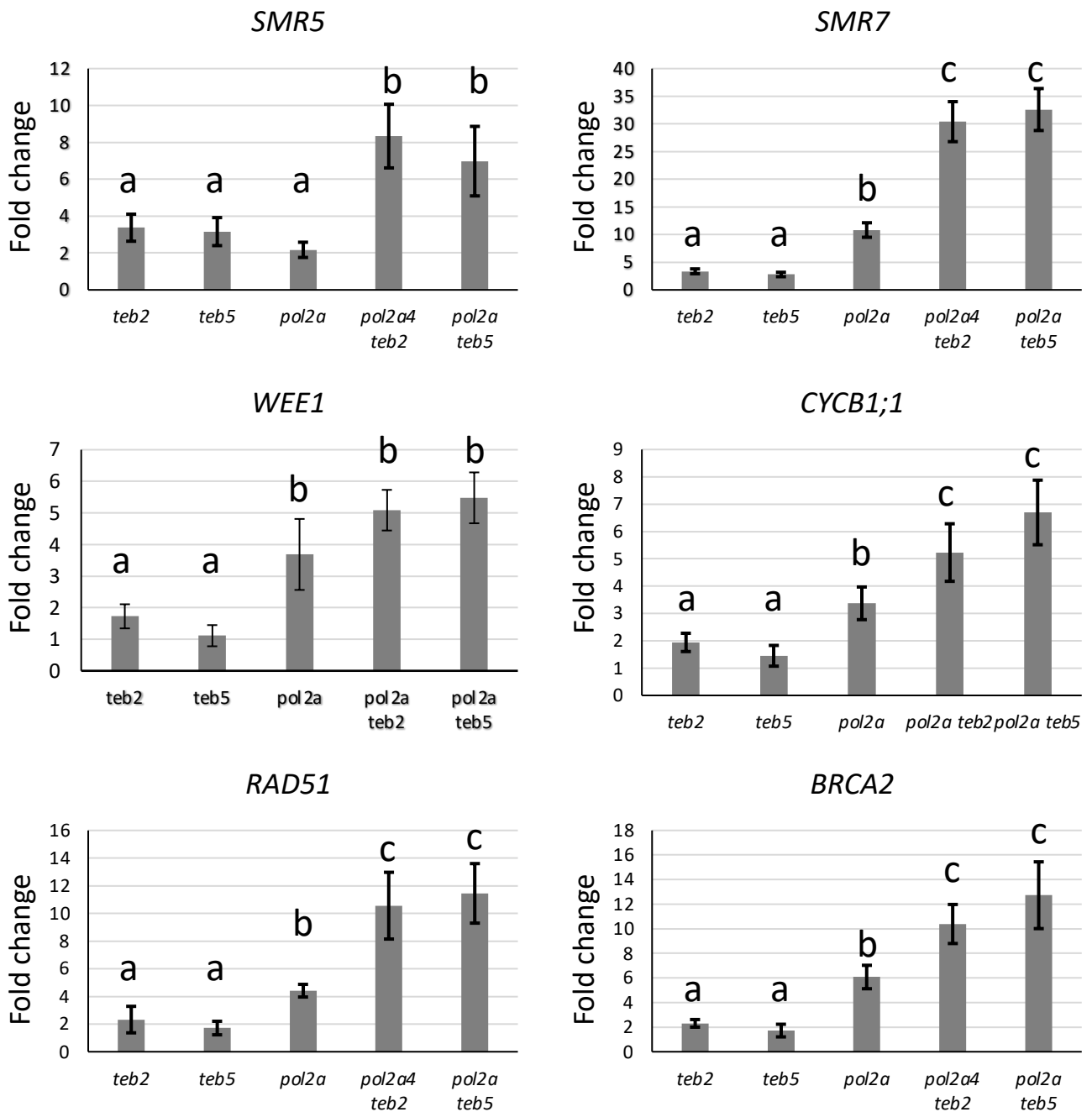


**Figure 5. DDR genes are hyper-induced in *teb pol2a* double mutants**

Total RNA was extracted from twelve-day-old plantlets. Expression of selected genes was assessed by real-time qPCR and normalized to actin. We monitored the expressions of genes involved in cell-cycle arrest (*SMR5*, *SMR7* and *WEE1*), DNA repair (*RAD51* and *BRCA2*) and both (*CYCB1;1*). Values are Fold change compared to the wild-type Col-0. Graphs represent average of 3 technical replicates +/- standard deviation and are representative of 3 independent biological replicates. Different letters above bars denote statistically relevant differences (ANOVA followed by Tukey test, performed on raw data before normalization,  $p < 0.01$ ).

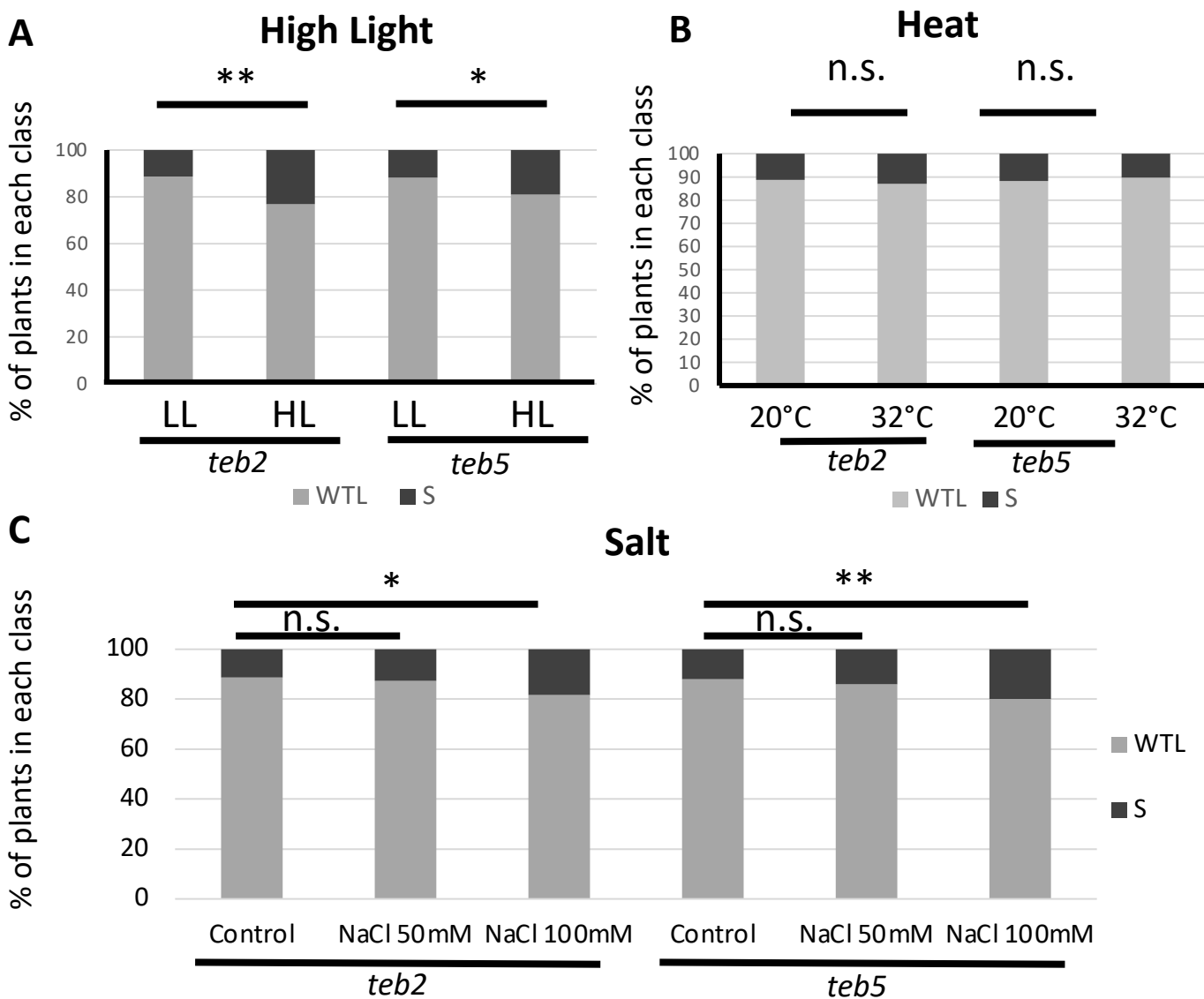


**Figure 6: Some abiotic stresses aggravate the developmental defects of *teb* mutants.**

A: Distribution of *teb* mutants between the different classes in plants grown in low light (LL,  $160\mu\text{mol} \times \text{m}^{-2} \times \text{s}^{-1}$ ) or high light (HL,  $350\mu\text{mol} \times \text{m}^{-2} \times \text{s}^{-1}$ ).

B: Distribution of *teb* mutants between the different classes in plants grown at standard temperature ( $20^{\circ}\text{C}$ ) or under heat stress ( $32^{\circ}\text{C}$ ). Plants were germinated *in vitro* and transferred to soil after 10 days. After 3 days of growth under control conditions at  $160\mu\text{mol} \times \text{m}^{-2} \times \text{s}^{-1}$  plants were kept under the same conditions or transferred to  $32^{\circ}\text{C}$  under the same light intensity.

C: Distribution of *teb* mutants between the different classes in plants watered with or without salt to the indicated concentration. Plants were germinated *in vitro* and transferred to soil after 10 days. After 3 days of growth under control conditions ( $160\mu\text{mol} \times \text{m}^{-2} \times \text{s}^{-1}$ ,  $20^{\circ}\text{C}$ , salt-treated plants were watered with a solution containing NaCl (50 mM), for the 100 mM treatment, salt concentration was increased to 100 mM after 2 days.

For all panels, n.s. indicates non-significant differences and asterisks denote statistically relevant differences between distributions ( $\chi^2$ -test,  $p < 0.01$ ). Blind scoring was performed on wild-type and *teb* mutants in all growth conditions, the proportion of severe phenotypes observed in wild-type plants was below 2%.

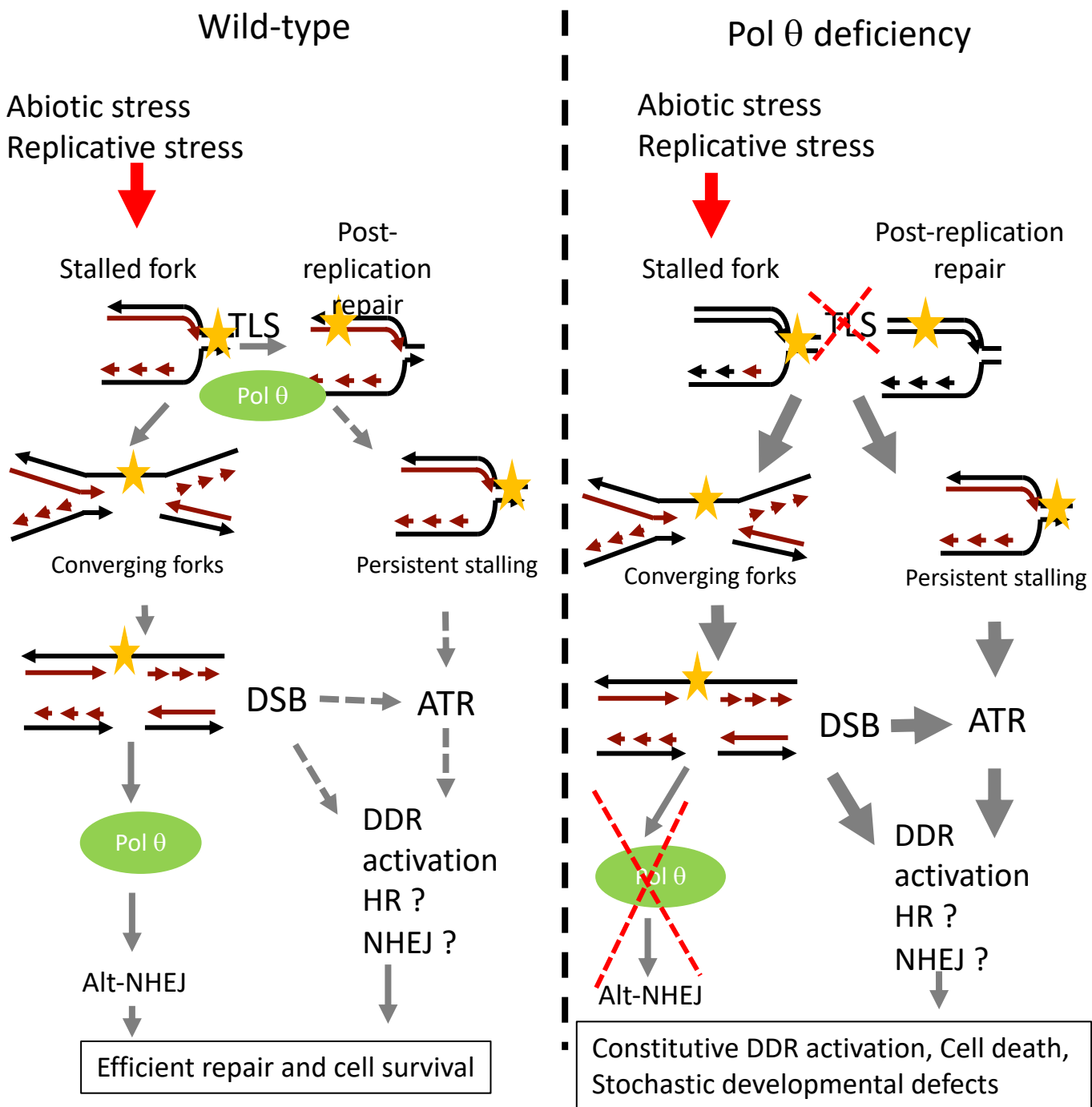


**Figure 7: Model for the role of Pol θ during replicative stress response**

**A:** In the wild-type, replication blocking lesions induce fork stalling. Pol θ can allow TLS through some lesions such as pyrimidine dimers. If efficient lesion bypass cannot be achieved, replisome disassembly and persistent fork stalling activates the DDR through ATR signalling, and DNA synthesis from a converging fork can lead to the formation of a double-ended DSB. Pol θ contributes to the repair of these lesions through Alt-NHEJ but other pathways such as HR or NHEJ likely contribute to DSB repair.

**B:** In the absence of Pol θ, TLS through some lesions is compromised, leading to an increased frequency of fork collapse and persistent stalling. Furthermore, Alt-NHEJ is also compromised, leading to an increased frequency of failed repair, constitutive activation of the DDR through ATR signalling, cell death and stochastic developmental defects. Abiotic stress and replicative stress can modify this equilibrium by enhancing the accumulation of more replication-blocking lesions, leading to an increased frequency of developmental defects in Pol θ deficient lines.

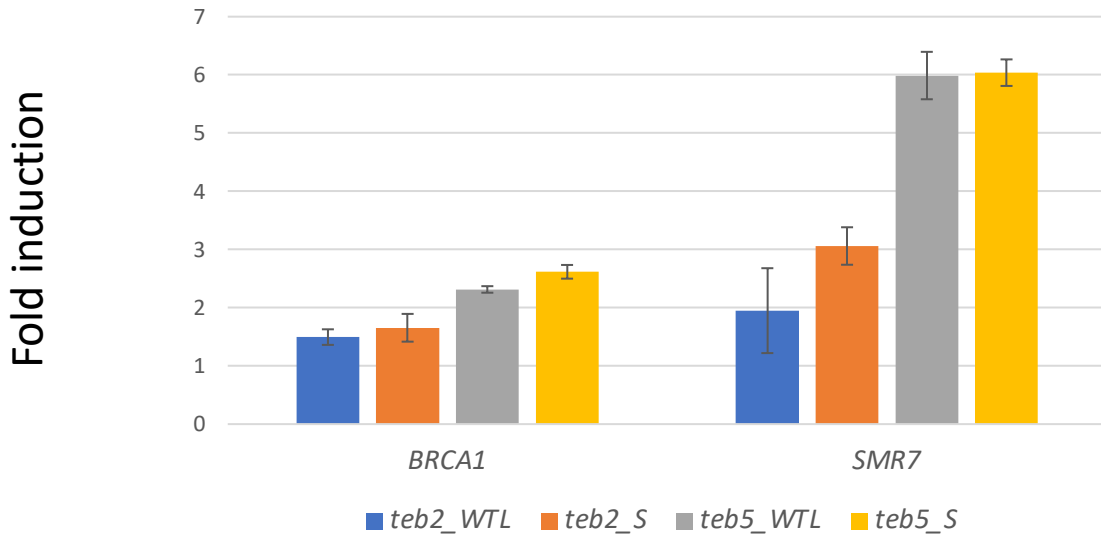


**Figure S1. Levels of DDR genes induction do not correlate with the severity of *teb* mutants' phenotype.** Expression of the DDR marker genes *BRCA1* and *SMR7* was monitored by qRT-PCR in rosette leaves of WTL and *S tebichi* mutants. Expression was normalized to that of *ACTIN*. Data are average +/- standard deviation of 3 technical replicates and representative of two independent experiments.

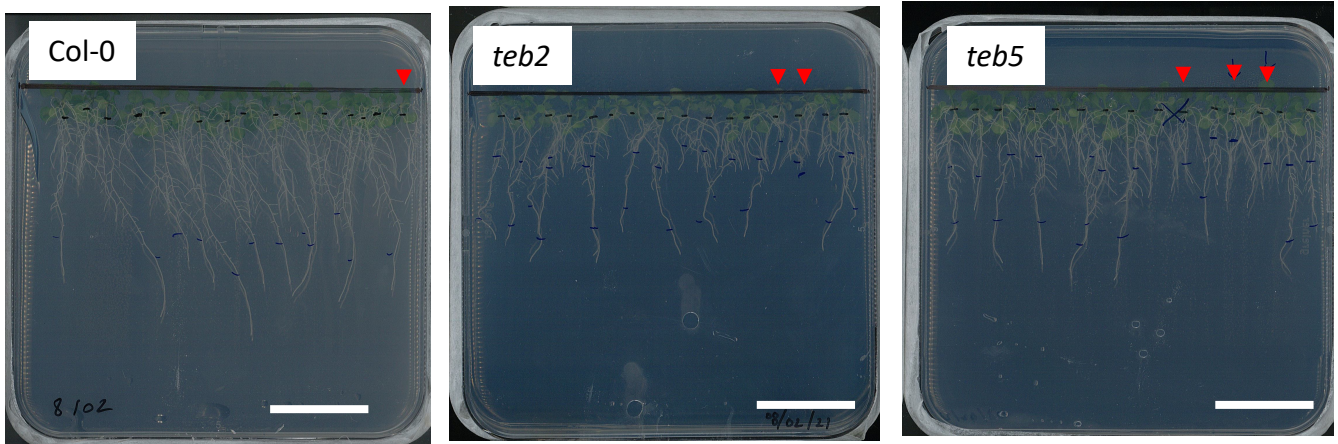


**Figure S2. Root growth defects show some heterogeneity in *teb* mutants**

Plantlets of the wild-type (Col-0) and *teb2* and *teb5* mutants were grown in vitro for 5 days, and aligned on half strength MS plates to be grown vertically. After 2 weeks, root growth of some plants appeared completely arrested in all genotypes (red arrowheads). The proportion of plants with arrested root growth was significantly higher in *teb* mutants (16% in *teb2* and 17% in *teb5*) than in the wild-type (7%),  $n = 75$  for all genotypes,  $\chi^2$  p-value < 0.001. Bar = 2cm for all pictures.



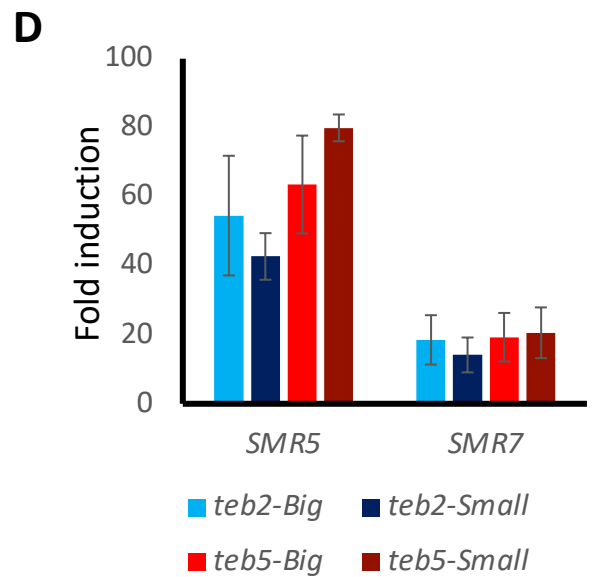
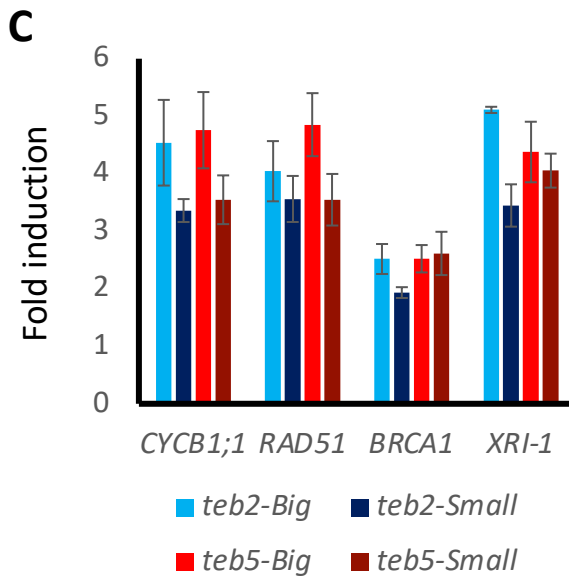
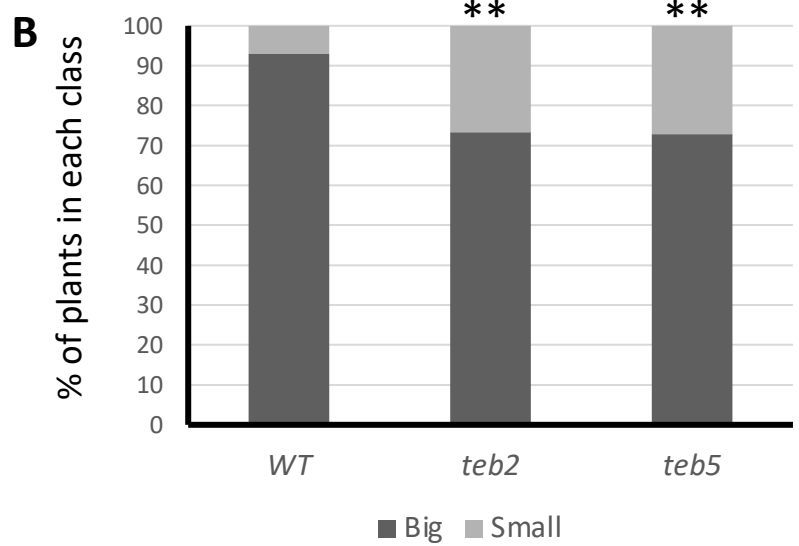


**Figure S3. Heterogeneous phenotypes of *teb* mutant plantlets do not correlate with different levels of DDR genes activation**

A: Representative picture of “big” and “small” plantlets observed among the *teb* mutants 10 days after germination, Bar = 500µm. B: Percentage of “big” and “small” plants among wild-type (WT) and *teb2* and *teb5* mutants (n>150 for all genotypes). \*\* denote statistically relevant differences  $\chi^2$  test p-value < 0.01. Data are representative for 3 independent experiments. C-D: qPCR analysis of DDR maker genes expression in small and big *teb* mutant plantlets. Expression levels were normalized using ACTIN as a reference gene, and results are expressed as fold-changed compared to the wild-type (Col-0). Data are average +/- standard deviation obtained from 3 technical replicates and are representative of 2 independent experiments.



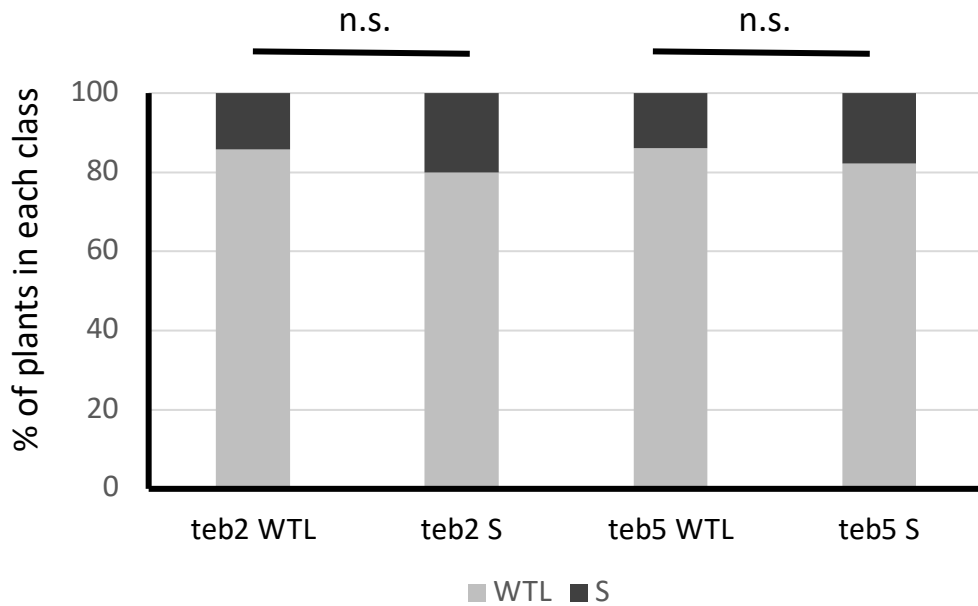


**Figure S4. The *teb* phenotype does not aggravate over generations**

Seeds from *teb* mutants with WTL and S phenotype were harvested and the distribution of individuals in each phenotypic category was estimated at the next generation. All three phenotypic classes were found in the progeny of each type of mutant, and no difference was observed in the distribution among the different classes between the three types of plants ( $\chi^2$ -test  $p > 0.05$ ).

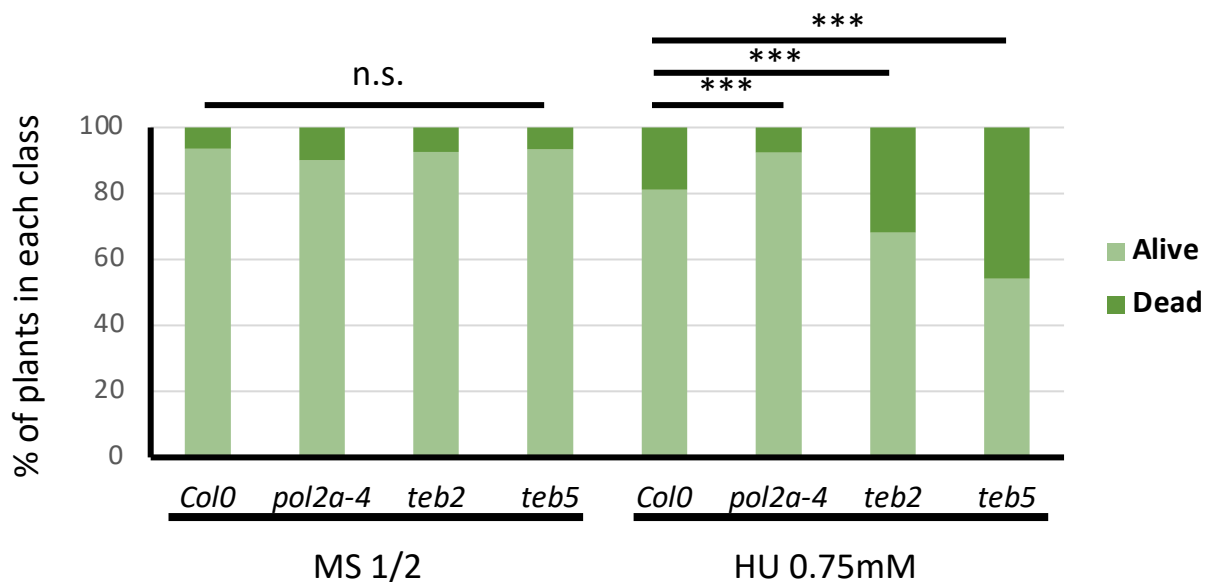


**Figure S5. *teb* mutants are hypersensitive to replicative stress**

Wild-type (Col0) and *teb* mutants (*teb2* and *teb5*) were germinated on MS supplemented or not with HU to a final concentration of 0.75mM. After 10 days, the survival rate was measured (n>100). While the survival rate on control medium was similar for all genotypes, *teb* mutants showed a higher proportion of dead plantlets ( $\chi^2$ -test,  $p < 0.001$ ). The *pol2a-4* that was shown to be tolerant to HU (Pedroza-Garcia et al, 2017) was used as a control.

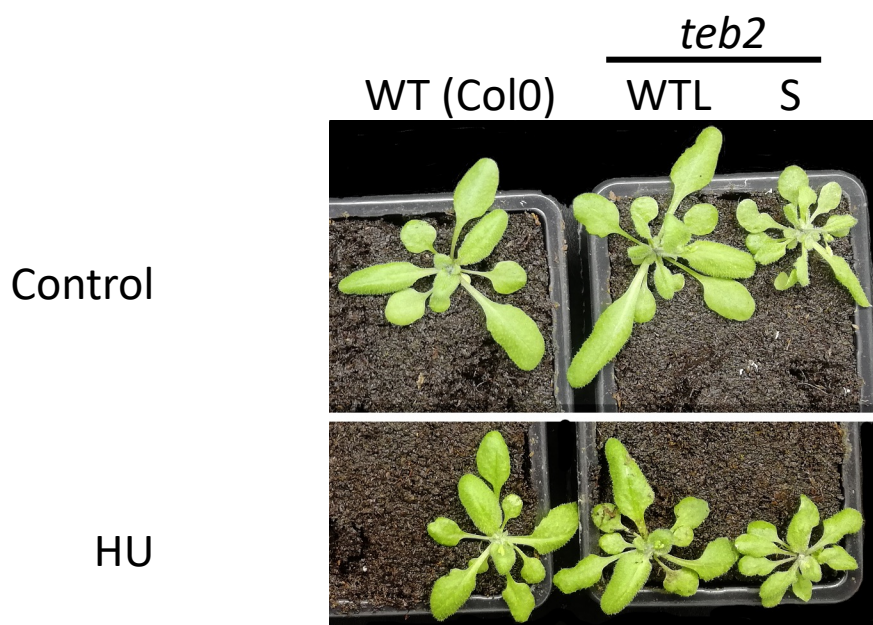


**Figure S6. Representative phenotypes of wild-type (Col0) and *teb* mutants exposed to HU before transfer to the green house**

Plants were grown for 10 days on half strength MS with or without HU (0.75mM). Surviving plants were transferred to the green house and grown for 3 weeks. Wild-type plants pre-treated with HU were slightly smaller than plants grown on MS alone. However, the characteristic *teb*-like phenotype was observed only amongst *teb* mutants.

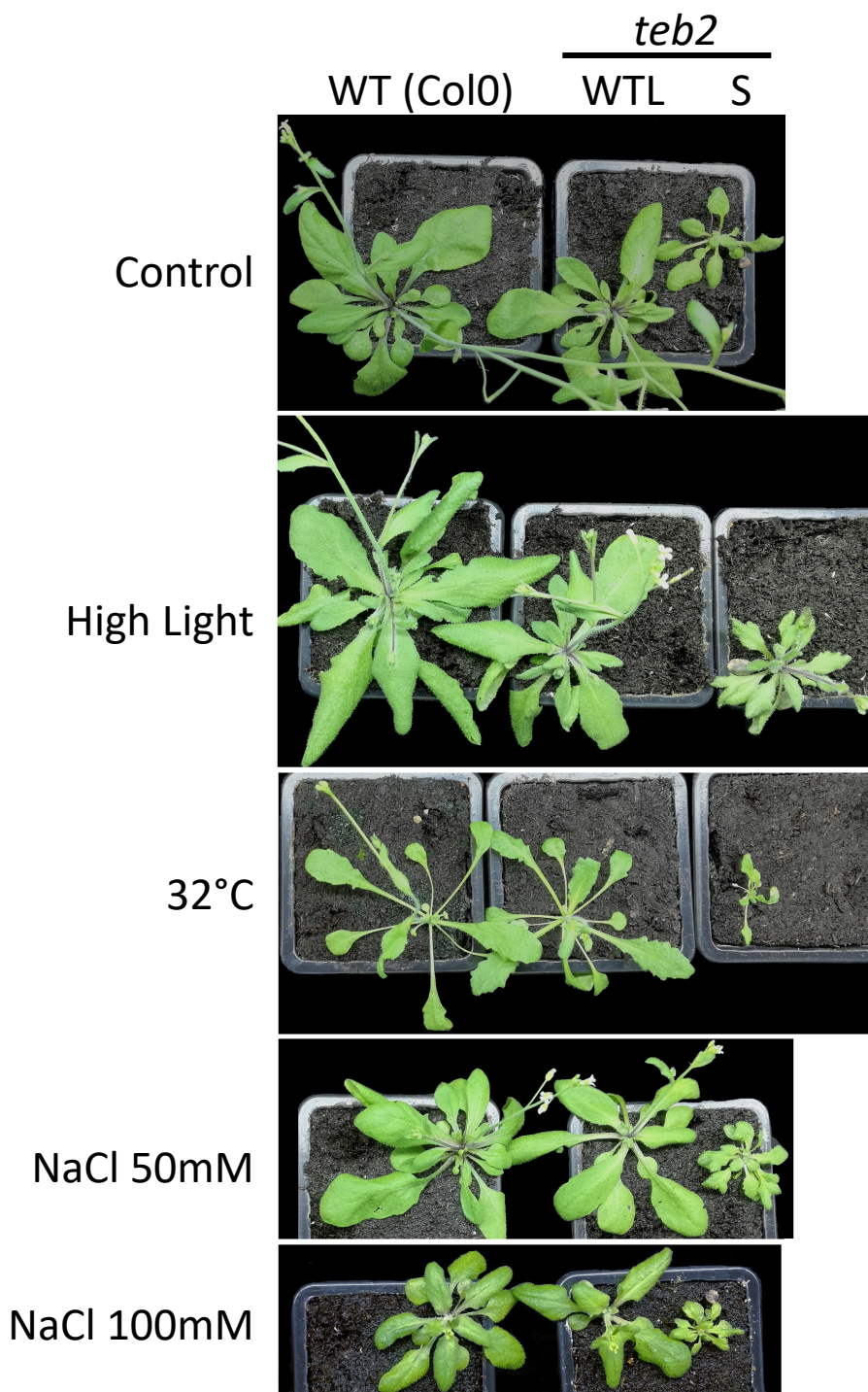


**Figure S7. Representative phenotypes of wild-type (Col0) and *teb* mutants grown under different conditions.**

Plants were grown for 1 month under the indicated conditions (see methods for details). Some of these growth conditions significantly altered the phenotype of wild-type plants: plants grown under high light were slightly larger with rolled leaves, plants grown at 32°C showed typical phenotype of plants acclimated to heat including elongated petiole and small leaf blade, while plants grown in the presence of salt showed reduced growth. The same modifications were observed in *teb* WTL plants. Moreover, none of these conditions induced the typical *teb*-like phenotype in wild-type plants.

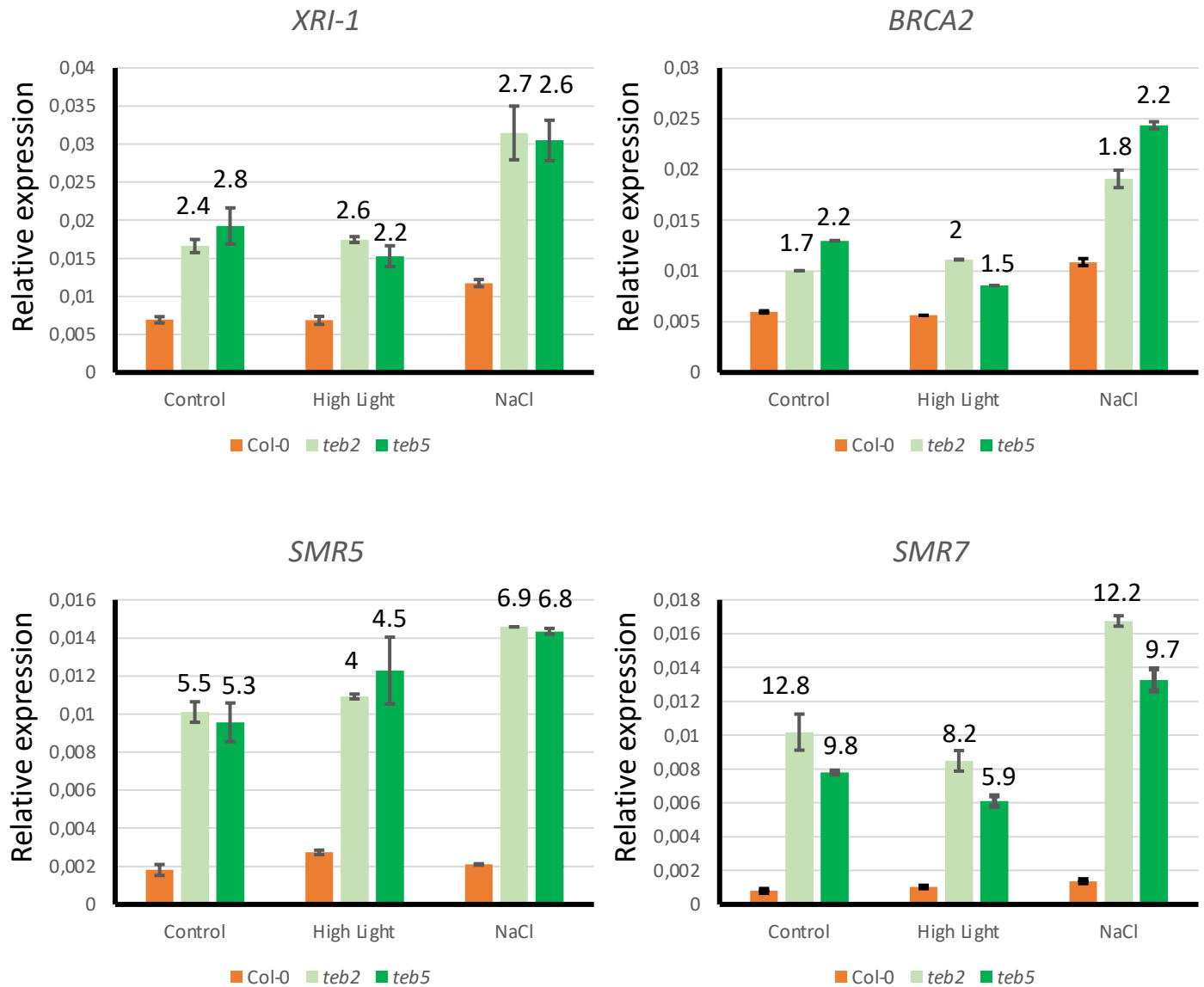


**Figure S8. Salt treatment, but not increasing light intensity activates DDR gene expression in both wild-type and *teb* mutants.**

Expression of DDR marker genes associated with DNA repair (*XRI-1* and *BRCA2*) or cell cycle arrest (*SMR5* and *SMR7*) was monitored by RT-qPCR in wild-type and *teb* mutants grown under standard conditions, germinated on NaCl supplemented medium (100mM) or exposed to high light. Data are average +/- S.D. obtained on 3 technical replicates and are representative of two independent experiments. They show relative expression of the selected genes compared to actin. Figures above bars represent the fold-induction compared to wild-type plants grown under the same conditions.